Bioorganic Chemistry 39 (2011) 73–87

Contents lists available at ScienceDirect

Bioorganic Chemistry

journal homepage: www.elsevier.com/locate/bioorg

Minireview

Manganese complexes displaying superoxide dismutase activity: A balance between different factors

Olga Iranzo *

Instituto de Tecnologia Química e Biológica, Universidade Nova de Lisboa, 2781-901 Oeiras, Portugal

ARTICLE INFO

Article history:
Received 28 December 2010
Available online 18 February 2011

Keywords:
Superoxide dismutases
Manganese complexes
SOD mimics
Superoxide radical

ABSTRACT

Superoxide radicals are one of the most toxic reactive oxygen species and its damaging effects lead to a variety of detrimental health conditions including cardiovascular diseases, neurodegenerative disorders and other types of age-related diseases. Following Nature example, chemists have designed manganese complexes that mimic the protecting action of the superoxide dismutases (SOD), metalloenzymes that catalyze the conversion of superoxide radical to the less toxic oxygen and hydrogen peroxide. This review provides an overview of the different SOD mimic manganese complexes developed mainly over the last decade, with particular attention to those factors that could be playing a crucial role in determining their activity.

© 2011 Elsevier Inc. All rights reserved.

Contents

1. Introduction

Many disease states affecting humans and many other mammals are the result of a failure to control and limit the overproduction of an undesired metabolic by-product. One example of these potentially harmful products are the reactive oxygen species (ROS). All mammals consume oxygen as the ultimate oxidant supporting cellular respiration and although the routine reduction of oxygen by the mitochondrial electron-transport chain to produce water is a relatively safe process, a considerable portion of the oxygen is metabolized through successive one-electron reduction reactions generating ROS [1]. One of these ROS is the superoxide radical ($O_2^{\cdot-}$), formed following a one-electron reduction of molecular oxygen (1–5% of the total oxygen consumed by humans is converted to $O_2^{\cdot-}$) [2,3]. This radical ion has both reducing and oxidizing properties, reacting mainly with metal ions and iron–sulfur clusters, and it can be readily converted to even more toxic species such as peroxynitrite (formed at diffusion controlled rates from the reaction of superoxide and nitric oxide radicals) [4,5], which is a strong oxidizing, nitrating and nitrosylating agent. Consequently, superoxide radicals are potentially dangerous for all cellular systems.

Superoxide dismutases (SODs) are metalloenzymes that catalyze the conversion of superoxide radical ($O_2^{\cdot-}$) to oxygen (O_2) and hydrogen peroxide (H_2O_2) at rates approaching the diffusion-controlled limit (Eq. (1)). Therefore, they play a crucial role in pro-

* Fax: +351 21 4411277.
E-mail address: oiranzo@itqb.unl.pt

0045-2068/$ - see front matter © 2011 Elsevier Inc. All rights reserved.
doi:10.1016/j.bioorg.2011.02.001

tecting biological systems against the damage mediated by this deleterious radical [2,3,6,7]. Since the identification of Erythrocuprein as a SOD, the first metalloenzyme to be classified as such [8], different metalloenzymes have been discovered that catalyze the same overall reaction. They use different metal ion cofactors and based on this, SODs can be classified into four major groups: Copper–Zinc SOD (CuZn-SOD), Manganese SOD (Mn-SOD), Iron SOD (Fe-SOD) and Nickel SOD (Ni-SOD) [3,9,10].

$$2O_2^{\cdot-} + 2H^+ \xrightarrow{SOD} H_2O_2 + O_2 \quad (1)$$

Mammals possess two different classes of SODs to keep the level of superoxide radicals under control: the CuZn-SOD which is present in the cytoplasm, nuclear compartments and in the inter membrane space of the mitochondria (SOD1) [11,12] or in extracellular space (SOD3) [13], and the Mn-SOD, that is located in mitochondrial matrix (SOD2) [14]. However, there are circumstances where the production of superoxide radicals is excessive and the endogenous SODs cannot eliminate them leading to a variety of disease states. In recent years, oxidative stress, defined as an impairment in the balance between generation and clearance of ROS by these and other antioxidant enzymes (such as catalase and glutathione peroxidase) has been implicated in a variety of degenerative processes, diseases, and syndromes [15–19]. Some of these include cardiovascular diseases; chronic and acute inflammatory conditions; central nervous system disorders, cancer and a variety of other age-related diseases. Evidence shows that the formation of superoxide radicals ($O_2^{\cdot-}$) is a common denominator associated with all these conditions [16]. Superoxide dismutase enzymes (SODs) have demonstrated therapeutic efficacy in animal models of some of these disease states including myocardial [20–22], cerebral ischemia–reperfusion injury [23–26], neurodegeneration [27], inflammation [28], and cancer [29,30]. Indeed, bovine CuZn-SOD preparations (Palosein® and Orgotein®) are available for the treatment of inflammatory diseases in horses and dogs, and have had limited use in humans (Orgotein®). The potential therapeutic application of the SOD enzymes for the treatment of human diseases faces several limitations; chiefly among them being the lack of oral activity, the immunogenicity when the SOD derives from non-human sources, short half-lives (they are quickly eliminated from the blood stream), the inability to gain access to the intracellular space of cells where the superoxide radical is produced, and manufacturing costs.

Considering the above, it is not surprising to see the interest of the chemistry community in developing low molecular weight catalysts that mimic the natural SOD enzyme's ability of eliminating superoxide radicals under physiological conditions. These types of molecules (SOD mimics) would be expected to have considerable therapeutic potential and could also become important probes to elucidate the physiologic and pathologic significance of the intracellular superoxide radical. Of the four metals found in the active center of the SODs and known to catalyze the disproportionation of superoxide radical to hydrogen peroxide and oxygen, manganese has been the preferred metal for the development of this type of complexes. The main reason for that is its low toxicity compared to the others metals since the free aquated metal ion Mn(II) is less prone to Fenton chemistry (to react with hydrogen peroxide and generate hydroxyl radical, Eq. (2)) [31–33]. Additionally, it has been shown that high intracellular Mn(II) concentrations can provide protection against oxidative stress [34–37]. Recently, studies by Culotta and coworkers show how Mn(II) can act as an antioxidant backup for the CuZn-SOD [38].

$$M^{n+} + H_2O_2 \rightarrow M^{(n+1)+} + OH^- + OH^{\cdot} \quad (2)$$

After a general overview of the native Mn-SOD and the different methods employed to measure SOD activity, this review will focus mainly on the development of manganese complexes that show SOD activity and therefore, have the potential of becoming new therapeutic agents for treatment of oxidative stress related diseases and/or important mechanistic probes. Understanding the reactions of superoxide radical with metal centers can help in gaining insights into the mechanism of action of the native SODs and conceiving whether and how metal complexes can be used as pharmaceuticals or mechanistic probes.

2. Native Mn-SOD

Mn-SODs (SOD2), first discovered by Fridovich and co-workers [39], are found in the mitochondria of eukaryotic cells and in the cytoplasm of many bacteria, typically as tetramers and dimers, respectively. These enzymes share a high degree of sequence and structural homology with the Fe-SODs, metalloenzymes found in prokaryotes and in the chloroplast of some plants [40,41]. Indeed, whereas the binuclear CuZn-SODs and Ni-SODs belong to different lineages, the Mn-SODs and Fe-SODs are evolutionary related. The active center of these enzymes contains a single Mn (or Fe) coordinated by two histidines and an aspartic acid in the equatorial plane, and a histidine and a solvent molecule in the axial positions forming a distorted trigonal bipyramidal geometry (Fig. 1). A hydrogen-bond network extends from the water bond molecule and comprises several residues, among them Gln143 and Tyr34 (based on human MnSOD sequence numbering). This network is postulated to play a crucial role in facilitating proton transfer upon reduction of the superoxide radical to H_2O_2 and, in particular Gln143, in controlling the redox potential of the metal center. The latter is a critical element for proper activity as explained later on. This active center is localized in an hydrophobic environment at the end of a tunnel where positively charged amino acids are postulated to provide electrostatic guidance for the approach of the superoxide radical (electrostatic tunneling) [10,42].

The overall mechanism by which these SODs catalyze the disproportionation of superoxide radicals has been called a "ping-pong" mechanism since the metal center, the redox active species, cycles between the oxidation states M(III) and M(II) with the subsequent oxidation and reduction of the superoxide radical (Eqs. (3a) and (3b) where M corresponds to metal). Metal reduction is coupled to proton uptake most likely by the coordinated solvent molecule (axial position in Fig. 1) that cycles between the hydroxo and aqua forms in the oxidized and reduced metal oxidation state, respectively [43,44]. The catalytic mechanism of Mn-and Fe-SODs is still a topic of discussion and different mechanisms have been proposed (see Refs. [9,10] for recent reviews).

$$SOD - M(III)(OH^-) + O_2^{\cdot-} + H^+ \rightarrow SOD - M(II)(OH_2) + O_2 \quad (3a)$$

$$SOD - M(II)(OH_2) + O_2^{\cdot-} + H^+ \rightarrow SOD - M(III)(OH^-) + H_2O_2 \quad (3b)$$

Net reaction:

$$2O_2^{\cdot-} + 2H^+ \rightarrow H_2O_2 + O_2 \quad (1)$$

Optimal SOD activity in aqueous solution requires redox potentials reasonably close to 0.36 V vs. Normal Hydrogen Electrode (NHE) (0.12 vs. Saturated Calomel Electrode, SCE), the intermediate value between the one-electron reduction potential for oxygen (−0.16 V vs. NHE, −0.40 V vs. SCE, pH 7.0) and the one-electron reduction potential of superoxide radical (0.89 V vs. NHE, 0.65 V vs. SCE, pH 7.0) [45]. This value is optimal for the disproportionation reaction since it allows for equal rate constant for each half reaction ($k_{cat} \approx k_{ox} \approx k_{red} \approx 2 \times 10^9$ $M^{-1}\,s^{-1}$) [46,47]. Consistent with this, the majority of redox potentials of SODs fall into the range of 0.2–0.45 V vs. NHE (Fig. 2) [46,48–51]. These enzymes illustrate very well how the protein scaffold proficiently fine-tunes

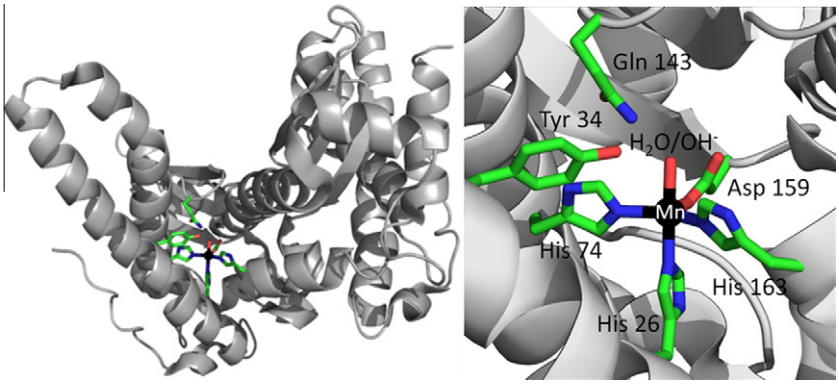

Fig. 1. Pymol representation showing (A) the Human mitochondrial Mn-SOD (PDB 1N0J) and (B) a close-up vision of the active metal center.

the redox properties of their metal center to achieve the required redox potential. What it is even more remarkable if one considers the different electronic and redox properties of manganese and iron, is the fact that both SODs, Mn-SOD and Fe-SOD, achieve a similar redox potential using practically the same active center [51]. However, with the exception of a small number of the so-called cambialistic SODs (active with either metal) [52–56], neither Fe-substituted Mn-SOD nor Mn-substituted Fe-SOD typically show catalytic activity [40,41,57–59]. This intriguing behavior has been proposed to be the result of an inappropriate metal redox potential. Recent reviews cover the research carried out towards the understanding of this fascinating metal ion functional specificity, summarizing interesting findings both at the level of native SODs and related synthetic models [51,60–62].

3. Determination of SOD activity

Several methodologies have been employed to determine the SOD activity and they can be divided mainly into two groups: direct and indirect methods.

3.1. Direct methods

They allow precise measurement of the catalytic rate constants for disproportionation of superoxide radicals since excess of superoxide radical over the SOD/SOD mimic can be utilized. They include two fast kinetic techniques: pulse radiolysis and stopped flow analysis. In pulse radiolysis, the superoxide radical is generated "in situ" very rapidly by pulse irradiation of oxygen saturated aqueous solution in the presence of formate. This fast production (sub-microsecond scale) allows a large time window for determining the reaction kinetics. The process of the reaction is monitored by UV–Vis spectroscopy following the changes in absorbance of the superoxide radical and/or transient species [63–65]. The stopped-flow methodology involves the rapid mixing of two solutions, one containing generally potassium superoxide in dimethyl sulfoxide (DMSO) and the other the SOD/SOD mimic in buffer (1:10–1:20 DMSO:buffer) or in DMSO containing a low amount of water (around 0.06%). The time-scale here falls into the milliseconds range (limited by mixing time). Monitoring is again performed using UV–Vis spectroscopy [66–68]. The requirement of DMSO medium could be criticized as being not a biological environment. However, it has been pointed out that aprotic media may represent more closely the "hydrophobic biological matrix" of organelles such as mitochondria [69], which indeed is the major source of superoxide radicals in aerobic organisms. Under less protic conditions, causing a longer half-life of superoxide radicals, efficient superoxide disproportionation is even more desirable.

3.2. Indirect methods

These assays are based on the competition between SOD/SOD mimic and an active redox indicator for superoxide radicals. Basically, upon reaction with the superoxide radical, the reporter molecule is reduced affording either a spectrophotometric or fluorescent change. A SOD/SOD mimic will therefore diminish the concentration of superoxide radical and the subsequent response of the indicator. Different sources and indicators of superoxide radicals have been used. The method most often employed, known as McCord-Fridovich (McCF), involves the enzymatic generation of

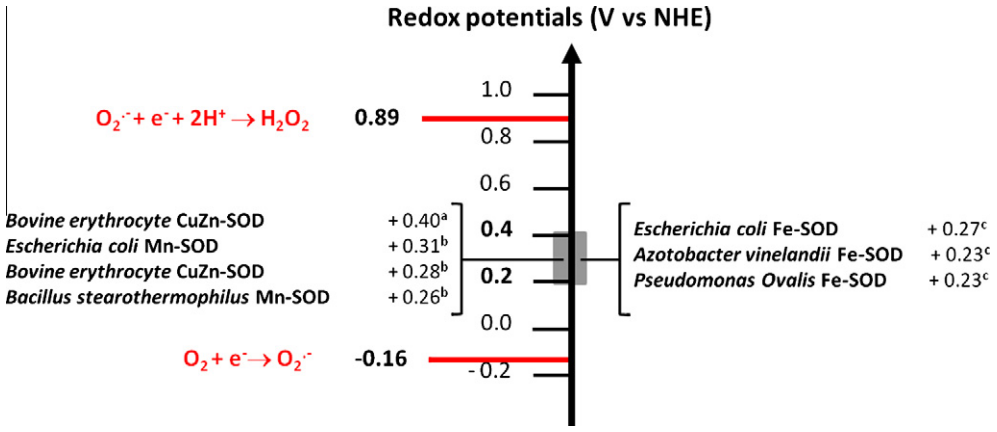

Fig. 2. Redox potentials for the reduction and oxidation of superoxide radical and for several SOD in aqueous solution at pH 7.0 ((a) Ref. [158]; (b) Ref. [48]; (c) Ref. [46]).

the superoxide radicals by the system xanthine/xanthine oxidase and the use of Cytochrome C (cyt *c*) or nitro blue tetrazolium (NBT) as indicators [8,70a]. Since the reduced form of NBT is only sparingly soluble in water, new tetrazoilum salts have been developed and are used as a reporters [71–73]. However, the important drawback of using NBT to determine SOD activity is the fact that NBT itself can mediate the formation of superoxide radicals [70b,c]. The spin trap 5,5-dimethyl-1-pyrroline 1-oxide (DMPO) has been also employed as an indicator in combination with electron paramagnetic resonance (EPR) spectroscopy [74]. Other types of indirect methods are those based on autooxidation reactions, where the scavenger molecule is both the source of superoxide radicals and the indicator. Organic substrates such as pyrogallol [75], 6-hydroxydopamine [76] or adrenaline [77] have been employed in these assays. Photochemically reduced flavins have been also employed to generate superoxide radicals. In these cases, NBT is normally used as indicator [78]. Recently, an alternative way of superoxide generation, namely gamma irradiation of an aqueous solution of ethanol using a ^{60}Co source, has been successfully applied in combination with soluble tetrazolium salts as indicators [79]. Usually, by indirect methods one determines the IC_{50} (concentration of SOD/SOD mimic that causes 50% of the inhibition of the indicator reduction by the superoxide radical). Although used as a feature characterizing the SOD activity of the SOD/SOD mimic, IC_{50} values strongly depend on the concentration of the detector used and are thus not appropriate for establishing comparison between values reported in the literature. However, when the rate constant for the reaction of superoxide radical with the indicator is known, it is possible to calculate a catalytic rate constant ($k_{cat(IC50)}$) from the measured IC_{50} value which will be independent of the indicator concentration. Namely, at the IC_{50} concentration the superoxide radical reacts with the indicator ($k_{indicator}$) and with the SOD/SOD mimic at the same rate [80–83]. Therefore, the following equation can be used:

$$K_{cat(IC\ 50)} = k_{indicator}[\text{indicator}]/IC_{50}. \quad (4)$$

Compared with the direct methods, the indirect assays are more commonly used to determine the SOD activity of SOD mimics due to their convenience. However, since the actual rate constant for the disproportionation of superoxide radicals cannot be directly determined, they present several inherent problems that could limit their ability to generate reliable rate data and often affect the interpretation of the results if they are ignored. Thus, special attention must be given to the following facts: (1) SOD mimics could be reacting with the indicator giving a positive result by simply reducing the reporter or a negative result by oxidizing the reduced reporter; (2) when using the xanthine/xanthine oxidase system, SOD mimics could also generate positive results by directly inhibiting the action of the enzyme; (3) SOD activity generates hydrogen peroxide and considering that redox-active complexes can react with this product, an apparent catalytic cycle may be observed as a result of hydrogen peroxide acting as either a reductant or an oxidant. Although sometimes catalase has been added to the reaction mixture to scavenge the hydrogen peroxide and avoid the above redox cycle, the best option would always be the direct study of the putative reactivity of the SOD mimic with the hydrogen peroxide. Considering all the above, parallel studies that will asses all these points should be carried out to unambiguously determine the SOD activity of any putative SOD mimic. Another important issue that must be taken into account when using the xanthine/xanthine oxidase system as a source of superoxide radicals is the fact that these radicals are being produced in a stationary state mode at low concentrations (about 10^{-11} M) and very often the amount of putative SOD mimic vs. substrate (superoxide radical) is larger [84,85]. In these cases, a false catalytic activity could be obtained if there is a fast stoichiometric reaction between the SOD mimic and the substrate.

4. Manganese SOD mimics

The challenge of this field is how to design appropriate ligands to form stable metal complexes at the same time that they allow the adequate platform for facilitating the redox cycle of the metal ion. The following chemical features must be realized if the designed manganese center has to catalyze the disproportionation of superoxide radical: (1) the metal ion redox potential has to lie between the potential for oxidation (−0.16 V vs. NHE) and reduction (0.89 V vs. NHE) of superoxide radicals (Fig. 2); (2) the manganese ion must be able to cycle between the Mn(III) and Mn(II) oxidation states faster than the rate of the spontaneous disproportionation of superoxide radical; (3) the ligand must have high affinity for both the reduced and oxidized state of the metal to obtain complexes that are stable under physiological conditions (avoid the release of metal during the redox cycling); (4) a minimum of one coordination site must be available for binding of the superoxide radical if an inner-sphere SOD catalytic pathway applies.

Diverse design strategies have been developed to obtain low molecular weight Mn-complexes that show SOD activity. Studies so far have focused on elucidating important structure activity relationships (SAR) for the catalytic disproportionation of superoxide radicals with special attention to the metal-centered redox potentials, the electrostatic properties and the hydrophobic environment around the metal site. Except for some family of manganese complexes, biological data (either *in vitro* or *in vivo*) are not always available although this practice is becoming more standard. As a consequence, if a lot of information has been already gathered regarding important factors to consider when designing SOD mimics and testing for their activity, little is still known regarding the action and the molecular mechanisms by which these SOD mimics might function *in vivo*. Indeed, recent studies carried out by different groups showed how manganese complexes previously demonstrated to have SOD activity *in vitro* were not able to (a) functionally substitute the SOD enzymes in SOD-deficient strains of *Escherichia coli* (*E. coli*) and *Saccharomyces cerevisiae* (*S. cerevisiae*) [86a], and (b) efficiently protect human lymphoblastoid cells against radiation-induced damage [86b]. These results highlight how crucial it is the purity of the manganese complexes used [86b,c] and the fact that *in vivo* studies do not always parallel the *in vitro* observed SOD activity most likely by mislocalization of the manganese complexes (they were not at the right cellular compartment where superoxide radicals were produced), inadequate concentration of the active form (not enough amount of the suitable chemical form to disproportionate the superoxide radicals) or loss of the metal (low stability). In the latter case, the complexes could be acting as simple manganese carriers and the observed SOD activity be the result of the action of manganese itself [79,87,88]. Clearly, to achieve a better understanding of the molecular basis by which SOD mimics might function and provide defense against oxidative stress will require a strong collaboration between chemists and biologists. Determining the key chemical properties of the SOD mimics which are responsible for the biological effect is fundamental, as well as detailed pharmacokinetic and toxicology data (which are also limited so far).

This section will mainly cover those manganese complexes that have been reported to react with superoxide radicals over the last decade, with emphasis on *in vitro* studies. Previous reviews cover research on this topic with emphasis on the use of manganese complexes, mainly porphyrin, salen and macrocyclic derivatives, to treat the conditions of oxidative stress related diseases (*in vivo* studies) [89–93].

4.1. Macrocyclic ligands

Riley and co-workers have employed a combination of molecular mechanics calculations and synthesis to generate different seven-coordinate Mn(II) SOD mimic complexes using the macrocycle 1,4,7,10,13-pentazazcyclopentadecane as a template ligand. This work, which has been the subject of several previous reviews [90,94,95], led to the discovery of the complex **M40403** (Fig. 3), the prototypical complex of the family. This Mn(II) SOD mimic catalyzes the disproportionation of the superoxide radical with a rate constant value of 1.64×10^7 M^{-1} s^{-1} (Table 1). Later studies carried out by the group of Anderson and collaborators indicated a value of 3.55×10^6 M^{-1} s^{-1} (see paragraph below and Table 1). The complex **M40403** showed therapeutic activity in animal models of inflammation and ischemia by protecting them against tissue damage [96,97]. This complex was introduced into human clinical trials in 2001 and has advanced to Phase II clinical studies in the USA [95,98]. Based on structure–activity relationship studies together with different kinetic and mechanistic studies, both in H_2O and D_2O, the authors stated that these type of Mn(II) complexes function via a catalytic cycle where the rate-determining step is the oxidation of Mn(II) to Mn(III), independently if an inner- or outer-sphere mechanism applies [95,99,100]. In both cases, a minimal barrier to electron transfer is needed and therefore, a good catalyst will be one in which the Mn(II) center is constrained in a geometry that promotes rapid electron transfer, i.e. the pseudo-octahedral geometry required by the Mn(III). It was postulated that the seven-coordinate Mn(II) complex (having a planar macrocyclic ligand conformation with two trans-axial substituents, normally chloride anions) must have enough conformational flexibility to reorganize from the planar into a folded conformation that will stabilize the necessary pseudo-octahedral geometry in the corresponding Mn(III) complex. Indeed, the ligand **M40401** that was designed to favor folding into an octahedral geometry once coordinated to Mn(II) showed a higher SOD activity while ligand **M40404**, lacking this ability, showed no measurable catalytic rate (Fig. 3, Table 1) [94,95,97]. Nonetheless, recent studies have questioned the crucial role of this high conformational flexibility in determining the degree of SOD activity. The water-exchange rate constants and their corresponding activation parameters, measured by temperature and pressure dependent ^{17}O NMR techniques [101–103], revealed that a sort of eight-coordinate transition state could exist and thus, an associative interchange substitution mechanism could be expected [103]. These results imply that this type of seven-coordinate Mn(II) complexes can remain in their planar conformation with no need for a six-coordinate intermediate. Indeed, later on and consistent with these observations, these authors have shown how seven-coordinate Mn(II) complexes of acyclic and rigid ligands are very efficient in catalyzing the disproportionation of superoxide radicals (see Section 4.4, Acyclic multidentate ligands). This group and coworkers have also demonstrated how two related Mn(II) pentaazamacrocyclic complexes, **Mn(pyane)Cl_2** and **Mn(pydiene)Cl_2** (Fig. 3), react with NO catalyzing its dismutation into NO^-/HNO and NO^+ species [104,105]. This results differs from previous reports where it was claimed that this type of cyclic polyamines selectively react with superoxide radical, lacking reactivity with NO [95]. Thus, authors speculate that the protective effect of Mn(II) pentaazamacrocyclic SOD mimics against oxidative stress may well be the result of their capacity to remove both superoxide radical and NO species, which subsequently will reduce the formation of the toxic peroxynitrite.

An alternative mechanism for the Mn(II) complexes **M40403**, **M40401** and **M40404** has been proposed recently by Anderson and co-workers where the rate of oxidation of Mn(II) is not the rate-determining step [106]. The similar Mn(III)/Mn(II) redox potentials determined for these complexes (0.525, 0.464 and 0.452 V vs. NHE for **M40403**, **M40401** and **M40404**, respectively) do not correlate with their different SOD activity (Table 1). UV–Vis spectroscopy and pulse radiolysis studies indicate the formation of an intermediate (described as $[Mn(III)(L)O_2]^+$, L = pentazamacrocyclic ligand) upon reaction of the seven-coordinate Mn(II)

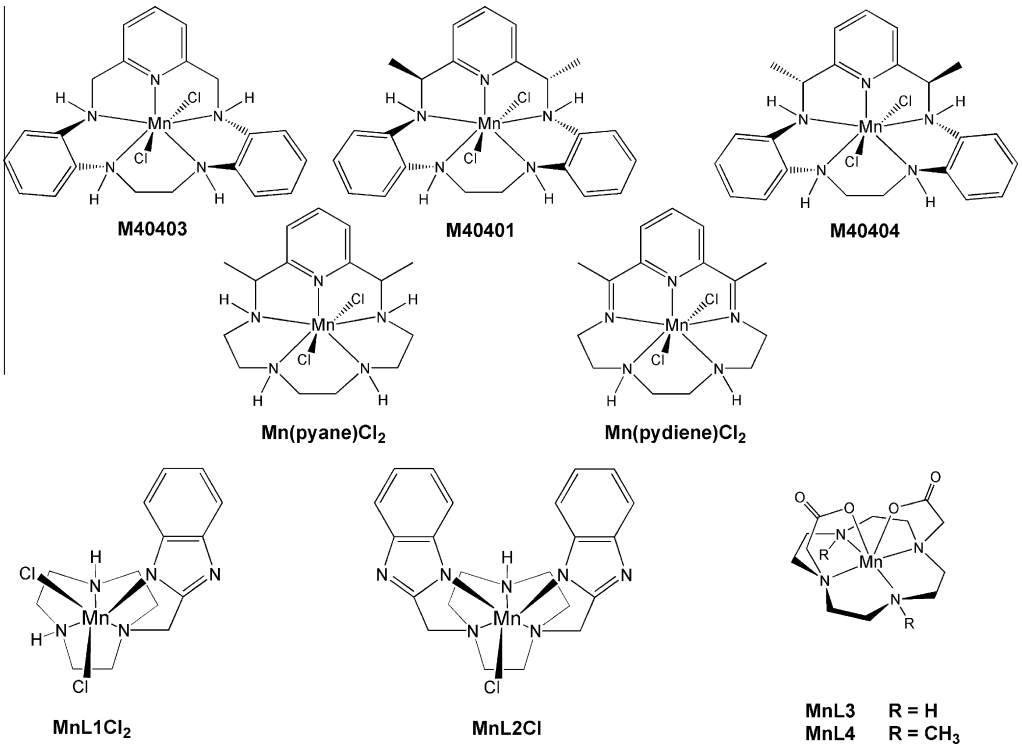

Fig. 3. Schematic of the manganese macrocyclic complexes.

Table 1
Redox potentials and SOD activity of different manganese complexes.

Complex	Redox potential[1]	SOD activity[2]				Ref.
	$E_{1/2}$ vs. NHE (solvent) (V)	IC_{50} (μM)	$K_{cat(IC50)}$[3] (M^{-1} s^{-1})	k_{cat} (M^{-1} s^{-1})	Method[4]	
Section 4.1. Macrocyclic ligands						
M40403	0.525 (ACN)[a]			1.64×10^7 (7.4) 3.55×10^6 (7.4) 2.6×10^6 (8.0)	S.-f. P.r.	[97] [106]
M40404	0.452 (ACN)[a]			Inactive	S.-f. P.r.	[95] [106]
M40401	0.464 (ACN)[a]			1.6×10^9 (7.4) 2.35×10^8 (7.4) 1.78×10^8 (8.0)	S.-f. P.r.	[97] [106]
MnL1Cl$_2$	0.392 (Water)[b]	8.33 (7.4)			Rb. (NBT)	[107]
MnL2Cl	0.769 (MeOH)[d] 0.939[c] (MeOH)[d]	5.36 (7.4)			Rb. (NBT)	[107]
MnL3	0.49[e] (Water)[f]	306 s[g]			McCF (NBT)	[108]
MnL4	1.15[h] (Water)[f]	390 s[g]			McCF (NBT)	[108]
Section 4.2. Salen derivatives/Schiff's base ligands						
EUK-8	− 0.13 (Water)[i]	1.3	6.0×10^5		McCF (NBT)	[110,88]
		1.3			McCF (cyt *c*)	[112]
		1.5			McCF (cyt *c*)	[158]
EUK-134		1.3	6.0×10^5		McCF (cyt *c*)	[112]
		1.54			McCF (cyt *c*)	[114,86b]
EUK-189		1.4	6.0×10^5		McCF (cyt *c*)	[112]
					McCF (cyt *c*)	[158]
MnL5		3.86			McCF (cyt *c*)	[114]
MnL6$_I$		0.62 (9.8)			McCF (cyt *c*)	[118]
MnL6$_{II}$		0.50 (9.8)			McCF (cyt *c*)	[118]
MnL6$_{III}$		0.55 (9.8)			McCF (cyt *c*)	[118]
MnL6$_{IV}$		0.54 (9.8)			McCF (cyt *c*)	[118]
MnL6$_V$		0.59 (9.8)			McCF (cyt *c*)	[118]
MnL6$_{VI}$		0.51 (9.8)			McCF (cyt *c*)	[118]
MnL7	−0.169[j] (Water)[k]	1.93 (7.4)	6.76×10^6		McCF (cyt *c*)	[119]
		1.70 (7.4)	9.10×10^6		McCF (NBT)	
[MnL8]$^-$	−0.0778[j] (Water)[l]	0.77	3.6×10^6		Rb. (NBT)	[120]
[MnL9]$^-$	−0.0471[j] (Water)[l]	1.14	2.4×10^6		Rb. (NBT)	[120]
[MnL10]$^-$	0.205[j] (Water)[l]	2.34	1.2×10^6		Rb. (NBT)	[120]
MnL11	0.425[j] (MeOH)[a] 0.360[j] (DMF)[a]	1.43	1.91×10^6		Rb. (NBT)	[121]
MnL12$_I$	0.327[j] (DCM)[d] 1.056[c,j] (DCM)[d]	0.29	4.09×10^7		McCF (NBT)	[122]
[MnL12$_{II}$]$^+$	0.285[j] (ACN)[d] 0.927[c,j] (ACN)[d]	0.39	3.04×10^7		McCF (NBT)	[122]
MnL13$_I$	0.341[j] (DCM)[d] 0.968[c,j] (DCM)[d]	Inestable in air				[122]
[MnL13$_{II}$]$^+$	0.410[j] (ACN)[d] 0.896[c,j] (ACN)[d]	1.12	1.06×10^7		McCF (NBT)	[122]
MnL14	0.143[j] (ACN)[d] 0.802[c,j] (ACN)[d]	0.76	1.56×10^7		McCF (NBT)	[122]
Section 4.3. Porphyrins/porphyrazines/phthalocyanine/biliverdins/corroles						
[MnT-4-PyP]$^+$	−0.200 (Water)[m]		3.4×10^4		McCF (cyt *c*)	[126]
[MnT-2-PyP]$^+$	−0.280 (Water)[m]		1.9×10^4		McCF (cyt *c*)	[126]
[MnTM-4-PyP]$^{5+}$	0.060 (Water)[m]	0.67	3.8×10^6		McCF (cyt *c*)	[127]
[MnTM-3-PyP]$^{5+}$	0.052 (Water)[m]	0.65	4.1×10^6		McCF (cyt *c*)	[127]
[MnTM-2-PyP]$^{5+}$	0.220 (Water)[m]	0.043	6.0×10^7		McCF (cyt *c*)	[127]
[MnTE-4-PyP]$^{5+}$	0.070 (Water)[m]		7.2×10^6		McCF (cyt *c*)	[126]
[MnTE-3-PyP]$^{5+}$	0.054 (Water)[m]		7.2×10^6		McCF (cyt *c*)	[130]
[MnTE-2-PyP]$^{5+}$	0.228 (Water)[m]	0.045	5.7×10^7		McCF (cyt *c*)	[125]
[MnCl$_1$TE-2-PyP]$^{5+}$	0.293 (Water)[m]	0.025	1.0×10^8		McCF (cyt *c*)	[124]
[MnCl$_2$TE-2-PyP]$^{5+}$	0.343 (Water)[m]	0.020	1.3×10^8		McCF (cyt *c*)	[124]
[MnCl$_3$TE-2-PyP]$^{5+}$	0.408 (Water)[m]	0.010	2.6×10^8		McCF (cyt *c*)	[124]
[MnCl$_4$TE-2-PyP]$^{5+}$	0.448 (Water)[m]	0.0065	4.0×10^8		McCF (cyt *c*)	[124]
[MnBr$_8$T-2-PyP]$^+$	0.219 (Water)[m]		4.3×10^5		McCF (cyt *c*)	[128]
[MnTPP]$^+$	−0.27 (Water)[m]		6.7×10^4		McCF (cyt *c*)	[126]
[MnPc]$^+$	−0.03 (Water)[m]		6.5×10^5		McCF (cyt *c*)	[126]
[MnT-2,3-PyPz]$^+$	0.09 (Water)[m]		2.9×10^6		McCF (cyt *c*)	[126]
[MnBM-2-PyP]$^{3+}$	0.05 (Water)[m]	0.78	3.3×10^6		McCF (cyt *c*)	[125]
[MnTrM-2-PyP]$^{4+}$	0.12 (Water)[m]	0.61	4.3×10^6		McCF (cyt *c*)	[125]
[MnTBAP]$^{3-}$	−0.194 (Water)[m]		1.45×10^3		McCF (cyt *c*)	[143]
[MnBV^{2-}]$_2$	−0.30 (Water)[m] 0.46[c] (Water)[m]	0.050	2.5×10^7		McCF (cyt *c*)	[88]
[MnBVDME]$_2$	−0.23 (Water)[m] 0.45[c] (Water)[m]	0.047	5.0×10^7		McCF (cyt *c*)	[88]
[MnMBVDME]$_2$	−0.26 (Water)[m] 0.44[c] (Water)[m]		2.3×10^7		McCF (cyt *c*)	[126]

Table 1 (*continued*)

Complex	Redox potential[1]	SOD activity[2]				Ref.
	$E_{1/2}$ vs. NHE (solvent) (V)	IC_{50} (μM)	$K_{cat(IC50)}$[3] (M^{-1} s^{-1})	k_{cat} (M^{-1} s^{-1})	Method[4]	
$[MnBVDT^{2-}]_2$	−0.26 (Water)[m]		2.5×10^7		McCF (cyt *c*)	[126]
	0.47[c] (Water)[m]					
MnL15	0.84[c] (Water)[n]	5.9	4.8×10^5		McCF (cyt *c*)	
				$<10^5$	P.r.	[145]
MnL16	0.91[c] (Water)[n]	3.2	8.7×10^5		McCF (cyt *c*)	[145]
MnL17	0.88[c] (Water)[n]	1.2	2.2×10^6		McCF (cyt *c*)	[145]
MnL18	0.76[c] (Water)[n]	1.5	1.8×10^6		McCF (cyt *c*)	[145]
				7.8×10^6	P.r.	
Section 4.4. Acyclic multidentate ligands						
$[Mn(TMIMA)_2]^{2+}$	0.64/0.28[o] (Water)[p]	1.6	3.6×10^6		McCF (cyt *c*)	[146]
[MnBMPG]$^+$	0.44/0.17[o] (Water)[p]	1.2	4.8×10^6		McCF (cyt *c*)	[146]
[MnIPG]$^+$	0.76/0.27[o] (Water)[p]	3.0	1.9×10^6		McCF (cyt *c*)	[146]
					P.r.	
			3.8×10^6			
[MnBIG]$^+$	0.76/0.33[o] (Water)[p]	3.7	1.5×10^6		McCF (cyt *c*)	[146]
					P.r.	
			1.4×10^6			
$[Mn(PI)_2]^{2+}$	0.34/0.20[o] (Water)[p]	0.87	6.6×10^6		McCF (cyt *c*)	[146]
[MnL19]$^+$	0.282/0.116[o] (Water)[q]	0.81	7.0×10^6		McCF (cyt *c*)	[148]
$[Mn(PhIIm)_2]^+$		1.26	4.1×10^6		McCF (cyt *c*)	[150]
$[Mn(PhI)_2]^+$		1.74	3.4×10^6		McCF (cyt *c*)	[150]
MnL20	−0.170[r] (DMF)[d]	2.93	9.3×10^5		Rb. (NBT)	[151]
$[MnL21]^{3+}$	−0.07 (DMF)[s]	3.3 (8.0)		9.3×10^5	McCF (XTT)	[152]
	0.51[c] (DMF)[s]	5.5 (8.0)		5.6×10^5	McCF (XTT)[t]	
$[MnL22]^{2+}$	0.37[j] (DMSO)[a]		1.2×10^7		S.-f.	[102]
					McCF (cyt *c*)	
		0.013	1.9×10^8			
MnL23	0.66[j] (DMSO)[a]		6.1×10^6		S.-f.	[153]
MnL24		29.9 (7.4)	3.8×10^5		McCF (NBT)	[83]
MnL25		24.7 (7.4)	4.6×10^5		McCF (NBT)	[83]
Section 4.5. Peptide-based ligands						
MnL26		8.08 (7.4)			McCF (NBT)	[157]

[a] 0.1 M Bu_4NPF_6 (Tetrabutylammonium hexafluorophosphate).
[b] 0.1 M $NaClO_4$.
[c] Half-wave redox potential for the Mn(IV)/Mn(III) couple.
[d] 0.1 M TBAP (Tetrabutylammonium perchlorate).
[e] Onset potential of the first observed oxidation peak, V vs. Ag/AgCl, KCl saturated.
[f] pH 7.0, 0.1 M KNO_3.
[g] Time required to oxidize 50% of NBT (maximum NBT oxidation was unchanged); control value = 294 s.
[h] Anodic potential, V vs. Ag/AgCl, KCl saturated.
[i] pH 7.9, 0.1 M NaCl.
[j] Half-wave redox potential vs. Ag/AgCl.
[k] 0.05 M KCl.
[l] 0.1 M KNO_3.
[m] 0.05 M Phosphate buffer, pH 7.8, 0.1 M NaCl.
[n] 0.01 M Phosphate buffer, pH 7.4.
[o] Anodic potential/cathodic potential V vs. SCE.
[p] 0.05 M Collidine buffer, pH 7.5.
[q] 0.05 M PIPES buffer, pH 7.5.
[r] Half-wave redox potential vs. SCE.
[s] 0.2 M Bu_4NBF_4 (Tetrabutylammonium tetrafluoroborate).
[t] In the presence of catalase.
[1] Half-wave redox potential for the Mn(III)/Mn(II) couple unless noted otherwise. Reference electrodes: NHE = normal hydrogen electrode, SCE = saturated calomel electrode, Ag/AgCl = silver/silver chloride electrode. For comparisons, these conversion factors can be employed to estimate values vs NHE: $E_{1/2} = E_{1/2}$, (SCE) + 0.2412; $E_{1/2} = E_{1/2}$, (Ag/AgCl) + 0.197 (Electrochemical Methods: Fundamentals and Applications, A.J. Bard and L.R. Faulkner, John Wiley & Sons, New York, 2nd Ed.). Solvent abbreviation: ACN = acetonitrile, MeOH = methanol, DMF = dimethylformamide, DCM = dichloromethane, DMSO = dimethyl sulfoxide.
[2] pH = 7.8 unless noted otherwise.
[3] Values determined from IC_{50}values using Eq. (4) in text.
[4] Pulse radiolysis = P.r.; Stopped-flow = S.-f.; McCord-Fridovich assay (indicator) = McCF (indicator); Riboflavin photoreduction assay (indicator) = Rb. (indicator).

complexes with the superoxide radical. This intermediate oxidizes the second superoxide radical molecule with subsequent reduction of the metal center. Authors claim that the SOD activity is governed by the geometry of the intermediate $[Mn(III)(L)O_2]^+$ and its reactivity with the second superoxide radical molecule, the step proposed as rate-determining in this catalytic cycle.

Using 1,4,7-triazacyclononane (tacn) as a template, Li and coworkers designed two new ligands wearing benzimidazole as a pendant arm: 1-(benzimidazol-2-yl-methyl)-tacn and 1,4-bis (benzimidazol-2-yl-methyl)-tacn [107]. These ligands coordinated to Mn(II) and the X-ray crystal structures show a six-coordinate Mn(II) ion bonded to the tacn ring, the nitrogen of the benzimidazole pendant arms and two chloride anions (**$MnL1Cl_2$**) or one (**MnL2Cl**) forming a distorted octahedron (Fig. 3). The pH titrations indicate that these Mn(II) complexes have good thermodynamic stability and kinetic inertness in aqueous solution. The electrochemical studies in methanol revealed a quasi-reversible Mn(II)/Mn(III) redox process for complex **$MnL1Cl_2$** (0.151 V vs. SCE, 0.392 V vs. NHE, Table 1) and two redox processes for **MnL2Cl** that correspond to the Mn(II)/Mn(III) and Mn(III)/Mn(IV) couples (0.527 V vs. SCE, 0.769 V vs. NHE and 0.697 V vs. SCE, 0.939 V vs. NHE, respectively; Table 1). Both complexes **$MnL1Cl_2$** and **MnL2Cl** showed SOD activity

at pH 7.4 with IC_{50} values of 8.33 μM and 5.36 μM, respectively. The addition of BSA (up to 0.2 mg/L) had no effect. Based on the redox potentials, the Mn(II)/Mn(III) pair seems to be responsible for the SOD activity. The higher hydrophobic environment created around the metal center in **MnL2Cl** (two benzimidazole arms) is postulated to be the origin of its higher activity relative to **MnL1Cl$_2$**. Catalase activity was also reported for these complexes and the overall low SOD activity of these Mn(II) complexes could be due to their conversion into OH- or O-bridged dinuclear Mn(III) or Mn(IV), favoring catalase vs. SOD activity.

Bencine and collaborators have used another polyazamacrocycle, the 1,4,7,10-tetraazacyclododecane (cyclen), to prepare two ligands (cyclen-1,7-diacetic acid and 4,10-dimethyl-cyclen-1,7-diacetic acid) [108]. These macrocycles bound Mn(II) with high affinity and six-coordinate Mn(II) complexes (**MnL3** and **MnL4**, Fig. 3) were postulated based on potentiometric pH titrations and similar reported systems. They showed high stability at physiological pH and temperature. No detectable release of Mn(II) was observed, even in a simulated environment reproducing the metal ion composition of biological fluids. Cyclic voltammetry experiments revealed irreversible redox processes with two broad overlapped oxidation peaks for **MnL3**, with an onset potential for first peak (assigned to a Mn(II) to Mn(III) process) of 0.49 V (vs. Ag/AgCl, silver/silver chloride electrode), and a single sharp oxidation peak for **MnL4** at 1.15 V (vs. Ag/AgCl). Further characterization of the latter revealed an oxidation process (Mn(II) → Mn(III)) whose rate is chemically controlled (rearrangement of metal coordination sphere to accommodate Mn(III) is slower than electron transfer) [109]. These complexes behave as superoxide radical scavengers since their high oxidation potentials and the irreversibility of the process preclude them of being SOD catalysts. They are capable of scavenging the superoxide radical generated by both exogenous (xanthine/xanthine oxidase/NBT, no interference observed with activity of xanthine oxidase) and endogenous (activated macrophages, RAW264.7 cells) pathways, being **MnL4** the more promising complex (effective in the nM–μM range). The authors showed how its activity correlates with its higher intracellular distribution. Further analysis of the pharmacological properties of **MnL4** reveals a safe toxicity profile, a decrease of the levels of oxidative stress key markers on cultured cells and a reduction of the anti-inflammatory effects in animal models of acute and chronic inflammation. Authors state that **MnL4** primarily acts as a superoxide radical scavenger not interfering with other inflammation-triggered metabolic pathways.

4.2. Salen derivatives/Schiff's base ligands

Manganese (III) salen derivatives have been developing as SOD mimics since it was shown by Malfroy, Jaconsen and coworkers that this type of complexes were able to exhibit SOD activity [110]. Work done until 1999 has been already reviewed and two compounds, **EUK-8** and **EUK-134** (Fig. 4), are considered the prototype molecules of this family of complexes [89,90]. They posses SOD (Table 1) and catalase activity, and substantial body of biological data suggest these Mn(III) salen complexes have protective effects in a range of disease models related to oxidative stress [89,111,112]. The replacement of the methoxy group in **EUK-134** by an ethoxy generated the complex **EUK-189**, a more lipophilic analog with similar SOD activity (Fig. 4, Table 1) [112]. Although the mechanism of action is not known, it is postulated that the origin of their biological effect is the result of the combination of both reactions, SOD and catalase. However, it should be noted that **EUK-8** and **EUK-134** have been reported to lose SOD activity in the presence of EDTA [86,93]. Paradoxically, prooxidant activity damaging free DNA has been reported but co-administration of either glutathione or alpha-lipoic acid was shown to inhibit it [113]. Giblin and coworkers developed a family of symmetrically and unsymmetrically substituted bipyridine analogs of **EUK-134** (based on the 6,6′-bis(2-hydroxyphenyl)-2,2′-bipyridine unit, Fig. 4) and obtained some Mn(III) complexes which enhanced catalase activity but lower SOD activity [114]. Specifically, the SOD activity of the best candidate (**MnL5**, Fig. 4) was 2.5 times lower than that of the parent **EUK-134** complex (259 Units/mM = IC_{50} of 3.86 μM

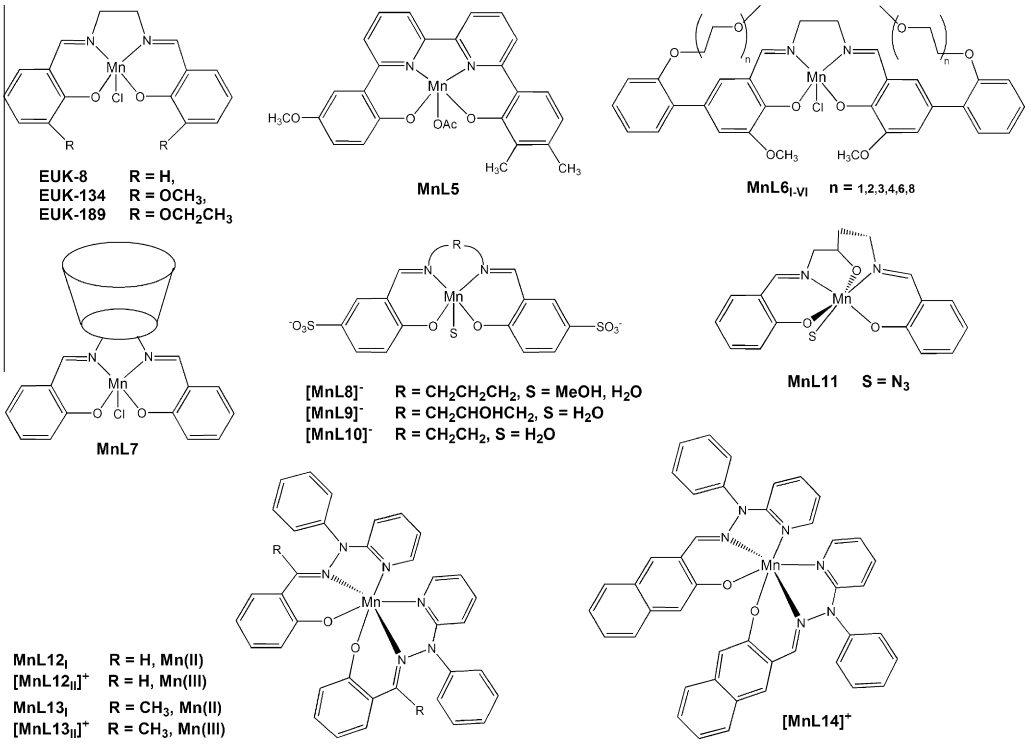

Fig. 4. Schematic of the manganese salen/Schiff's base derivatives complexes.

vs. 650 Units/mM = IC_{50} of 1.54 μM, where 1 Unit refers to one International Unit for SOD activity, Table 1) under the same experimental conditions. Later on, two new series of **EUK-8** analogs were designed by Doctrow and coworkers by either modifying the salen ring or the ethano bridge [115]. In this case, all the complexes showed comparable SOD activity (mean IC_{50} value of 0.7 μM) but increased catalase activity with the derivatives containing symmetrical 3- and 5-alkoxy substituents showing the best cytoprotective activity protecting cultured cells from hydrogen peroxide. Some complexes also showed neuroprotective activity in a rodent stroke model. No metal redox potentials were reported for any of these new series of complexes and thus no relationship can be established between their activity and their redox properties. It was observed that these complexes get commonly inactivated under the catalase assay conditions, most likely through the formation of higher oxidation species, and their SOD activity decreases in the presence of EDTA (Bovine serum albumin seems not to affect their SOD activity), being indicative of the loss of Mn(II). To increase the stability, Baudry and collaborators introduced a polyethylene glycol (PEG) modification in the positions 3 and 3′ of the ligand **EUK-134** to generate the cyclic ligand **EUK-207** [116]. The corresponding Mn(III) complex showed increased biological stability and similar SOD and catalase activities [117]. This type of modification was also used by the group of Lim who PEG-ylated the 5 and 5′ positions of **EUK-134** obtaining Mn(III) complexes (**MnL6$_{a-f}$**, Fig. 4) which SOD activities were 2- to 3-fold higher (IC_{50} = 0.50–0.62 μM, Table 1) [118].

The general low water solubility of manganese (III) salen derivatives complexes has prompted the development of new ligands. Vecchio and coworkers modified the structure of **EUK-8** to improve its water solubility properties by introducing a cyclodextrin unit [119]. The resulting Mn(III) complex (**MnL7**) showed good solubility in water and a slightly better SOD activity than the **EUK-8** complex under the same experimental conditions (1.93 vs. 2.46 μM (cyt *c*), 1.70 vs. 2.10 μM (NBT), Table 1). However, its catalase activity was decreased. The redox potential for the Mn(III)/Mn(II) couple became a little more positive than that of the parent complex (−0.169 V vs. −0.187 V vs. Ag/AgCl). Interestingly, the reoxidation step seemed to be partially allowed suggesting that the reduced species could either be decomposing or undergoing a partial ligand–metal dissociation process. It is worthy to note that the values reported in this study for the redox potential and SOD activity of **EUK-8** were determined under different conditions that those shown in Table 1. A different strategy was employed by Signorella and coworkers that introduced sulfonato groups in the salicylic unit obtaining the ligands 1,3-bis(5-sulphonatosalicylidenamino)propane (L8) and 1,3-bis(5-sulphonatosalicylidenamino)propan-2-ol (L9) [120]. They coordinate Mn(III) in a tetragonal environment as previous salen analogs with the ligand arranged in the equatorial plane (Fig. 4). The alcohol group present in the propane backbone of ligand L9 does not participate in metal coordination and although it seems not to have an effect on the overall geometry of the complex, it affects the Mn(III)/Mn(II) metal redox potential (quasi-reversible redox processes, −0.0471 V and −0.0778 V vs. Ag/AgCl for **[MnL9]**$^-$ and **[MnL8]**$^-$, respectively). Both complexes showed SOD activity with IC_{50} values of 1.14 (**[MnL9]**$^-$) and 0.77 (**[MnL8]**$^-$) μM. The corresponding calculated $k_{cat(IC50)}$ values are 2.4×10^6 and 3.6×10^6 M^{-1} s^{-1}. The Mn(III) complex of the related ligand 1,2-bis(5-sulphonatosalicylidenamino)ethane (**[MnL10]**$^-$) had a redox potential value of 0.205 V (vs. Ag/AgCl) and SOD activity with an IC_{50} of 2.34 μM (Table 1). For this series of complexes, the higher the metal redox potential, the lower the SOD activity is. This fact reveals a catalytic cycle where the oxidation of the metal should be the rate-determining step (this trend is also observed for some porphyrins and acyclic multidentate ligands, see Sections 4.3 and 4.4). These complexes showed also catalase activity. Recently, this group has demonstrated how the use of the asymmetry bridging linker 2-butanol generates a ligand (1,4-bis(salicylidenamino)butan-2-ol) that acts as a pentadentate unit stabilizing Mn(IV) instead of Mn(III) (**MnL11**, Fig. 4) [121]. In methanol and dimethylformamide the complex converted to the corresponding Mn(III) in equilibrium with its dimer and two redox processes were observed in these media: one quasi-reversible oxidation wave at 0.425 (methanol) and 0.360 (dimethylformamide) V vs. Ag/AgCl corresponding to the couple Mn(III)/Mn(IV), and another nonreversible reduction wave at around −0.450 (methanol) and −0.400 (dimethylformamide) V vs. Ag/AgCl corresponding to the couple Mn(III)/Mn(II). Similar behavior is also observed for Mn(III) porphyrin complexes, see Section 4.3. The redox potential for Mn(III)/Mn(II) is too negative and thus, the SOD activity observed at pH 7.8 (IC_{50} = 1.43 μM, $k_{cat(IC50)}$ = 1.91×10^6 M^{-1} s^{-1}, Table 1) is the result of the accessibility of the Mn(IV) oxidation state allowing the complex to redox cycle between Mn(III)/Mn(IV) and disproportionate the superoxide radical. Catalase activity is also reported for this complex.

The group of Ghosh have synthesized tridentate Schiff's base ligands containing a phenolato and a pyridine donor in addition to the imine group [122]. In all cases, bis complexes were obtained (**MnL12**, **MnL13** and **MnL14**, Fig. 4), however while the L12 and L13 coordinated to both Mn(II) and Mn(III), ligand L14 was only capable of stabilizing Mn(III). The X-ray crystal structure of **MnL12$_I$** and **[MnL12$_{II}$]$^+$** revealed a manganese ion coordinated to two ligands in a distorted octahedral fashion. Two redox waves were detected for each complex, one in the range 0.14–0.40 V vs. Ag/AgCl that was ascribed to the Mn(II)/Mn(III) couple, and a second one in the range 0.80–1.06 V vs. Ag/AgCl ascribed to the Mn(III)/Mn(IV) couple. The first set of values is appropriated for SOD activity and thus, all the complexes, with the exception of **MnL13$_I$**, showed activity with IC_{50} values ranging from 0.29 to 1.12 μM (Table 1). The complexes **MnL12$_I$**, **[MnL12$_{II}$]$^+$** and **[MnL13$_{II}$]$^+$** showed also nuclease activity in the presence of hydrogen peroxide.

4.3. Porphyrin and corrole derivatives

Manganese porphyrins were introduced as SOD mimics more than 30 years ago when a study, by Pasternack and co-workers, showed that the Mn(III) tetrakis(4-N-methylpyridyl)porphyrin complex had SOD activity (**[MnTM-4-PyP]$^{5+}$**, Fig. 5) [123]. Since then, Fridovich, Batinić-Haberle, Spasojević, Rebouças and coworkers have pioneered the development of manganese complexes of substituted porphyrins and have optimized their properties to achieve compounds with potency approaching that of the SOD enzymes. Recent reviews cover in detail this work thus, this section will give only a general overview [93]. To understand the structure activity relationships (SAR) that govern the SOD activity of these compounds, these groups studied the correlation between the metal-centered redox potential and the rate constant for the disproportionation of $O_2^{\cdot-}$ (k_{cat}) for different Mn(III) porphyrins (P), phthalocyanines (Pc), porphyrazines (Pz) and biliverdin IX (BV) derivatives (Fig. 5, Table 1) [88,124–126]. The rate constants were determined at pH 7.8 and 25 °C by competition kinetics using cyt *c* as the reference. All the cyclic voltammograms showed reversible or quasi-reversible redox waves, ascribed to the Mn(III)/Mn(II) or Mn(III)/Mn(IV) redox couple. For the first three type of ligands, the log k_{cat} increases linearly with the Mn(III)/Mn(II) redox potential $E_{1/2}$, predicting a 10-fold increase in k_{cat} for a 120 mV increase in redox potential, observation that is in agreement with the Marcus equation for outer-sphere electron-transfer reactions. Metal reduction is considered the rate-limiting step and the more positive the potential, the easier the reducibility of the Mn(III) complexes and the better the ability to disproportionate the superoxide radical.

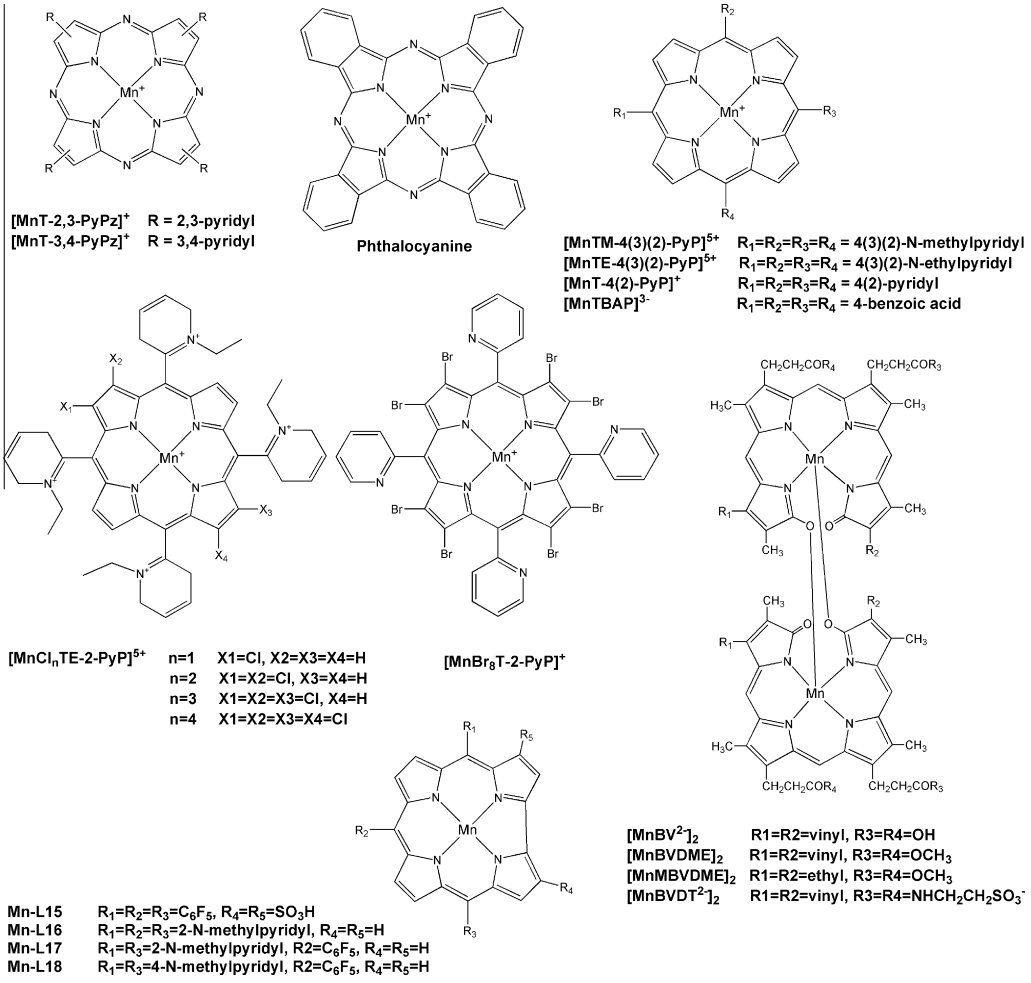

Fig. 5. Schematic of the manganese porphyrin/corrole derivatives complexes.

Ortho N-alkylpyridiniumyl porphyrins are more potent SOD mimics than the para and meta derivatives, reflecting their higher electron withdrawing power. However, as the +2 oxidation state is stabilized (series **[MnCl$_n$TE-2-PyP]$^{5+}$**, Fig. 5 and Table 1), the SOD activity of the metal complex increases at expenses of their stability and some of the complexes are not very stable under physiological conditions [124,126]. Complexes with very negative Mn(III)/Mn(II) redox potentials ($E_{1/2}$ < −190 mV vs. NHE) show very low or none SOD activity [125,126]. Despite their favorable redox potentials and SOD activities, only the ortho and meta isomers significantly protected SOD-deficient *E. coli* and allowed growth in an aerobic minimal medium. Previous work showed that the lower toxicity of these isomers compared to the para is related to their lower DNA binding affinity [127]. A different behavior is observed for the biliverdin IX derivatives that, due to their coordination properties (dimer structures, **[MnBV^{2-}]$_2$**, **[MnBVDME]$_2$**, **[MnMBVDME]$_2$**, **[MnBVDT^{2-}]$_2$**, Fig. 5), stabilize the Mn(IV) oxidation state. As a consequence, the Mn(III)/Mn(IV) oxidation occurs at potential values (0.44–0.47 V vs. NHE, Table 1) appropriate for the disproportionation of the superoxide radical while those for the Mn(III)/Mn(II) couple are too negative (Table 1) to catalyze the reaction [88,126]. Similar redox behavior is also observed for corrole complexes (see below). All these complexes showed SOD activity with $k_{cat(IC50)}$ ranging from 2.3 to 5×10^7 M^{-1} s^{-1} (Table 1). Due to their pentacoordinate geometry, the Mn(III) biliverdin complexes are inert towards nitric oxide and hydrogen peroxide what makes these complexes more selective towards superoxide radicals than porphyrins known to be reactive towards those species. Mn(III) biliverdin complexes are also efficient SOD mimics *in vivo* facilitating the aerobic growth of SOD-deficient *E. coli*.

Later on, this SAR was refined to account for the effect of electrostatics and charge distribution and differently charged/sized Mn porphyrin complexes were studied [87,128,129]. In addition to the appropriate redox potential, the presence of positive charges and their close placement and distribution related to the metal center (ortho vs. meta/para, in-plane or below/above the porphyrin ring) was found to be essential for the electrostatic facilitation of the disproportionation of superoxide radical. This explain cases where despite similar redox potentials very different SOD activities were observed (Table 1): penta-charged Mn(III) meso-tetrakis(N-ethylpyridinium-2-yl)porphyrin (**[MnTE-2-PyP]$^{5+}$**, $E_{1/2}$ = 0.228 V vs. NHE; $k_{cat(IC50)}$ = 5.7×10^7 M^{-1} s^{-1}) vs. singly charged Mn(III) beta-octabromo meso-tetrakis(2-pyridyl)porphyrin (**[MnBr$_8$T-2-PyP]$^+$**, $E_{1/2}$ = 0.219 V vs. NHE; $k_{cat(IC50)}$ = 4.3×10^5 M^{-1} s^{-1}) [128]. These results highlight the importance of mimicking the electrostatic tunneling of the SOD enzymes themselves and how both electrostatics and the spatial placement of the positive charge should be considered as crucial factors in the design of SOD mimics. Deviations of the Marcus plot are also observed for a series of Mn(III) meso-tetrakis(N-alkylpyridyl)porphyrins (alkyl being methyl, ethyl, *n*-propyl, *n*-butyl, *n*-hexyl, and *n*-octyl) where despite the favorable increase of the redox potential with the increase in chain length ($E_{1/2}$ from 0.220 to 0.367 V vs. NHE), a "V" shape dependence was observed for log $k_{cat(IC50)}$ vs. $E_{1/2}$ [130]. The rate constant decreases from methyl (log $k_{cat(IC50)}$ = 7.79) to *n*-butyl (log $k_{cat(IC50)}$ = 7.25) and then increases to *n*-octyl (log $k_{cat(IC50)}$ =

7.71). This behavior originates from interplay of solvation and steric effects that modulate electronic effects.

Overall, all these SAR studies revealed that for the Mn(III) porphyrin and derivatives with lower redox potential ($E_{1/2}$), the reduction of the Mn(III) is the rate-determining step in the catalytic reaction. Thus, the higher the redox potential, the higher the SOD activity is. However, further increase on the redox potential leads to the stabilization of the Mn(II) oxidation state and indeed to the formation of the corresponding Mn(II) complexes. From this point, the oxidation of the Mn(II) complexes becomes the rate-determining step and the k_{cat} value starts to decrease as the redox potential increases [93,131,132]. This trend is observed for other families of manganese complexes (see Sections 4.2 and 4.4).

Regardless the charge and fairly hydrophilic nature of these manganese porphyrins, several of them have already exerted remarkable protective effects in both *in vitro* and *in vivo* models of oxidative stress injuries where ROS are involved [93,129,130,132–136]. Further studies along these lines were focused on the design of new manganese porphyrins with tailored lipophilicity to improve cell uptake [137]. Recently, they have shown how enhanced lipophilicity can compensate for lower potency resulting in similar protection of SOD-deficient *E. coli* [138]. Some of these studies have proved that increasing the lipophilic character of the ligand can enhance *in vivo* efficacy by improving their bioavailability and entry in the cell. However, this could happen at expenses of an increase in toxicity since as the lipophilic character raises, their surfactant character becomes larger (toxicity) [132–134]. Another aspect researchers are trying to improve is their oral bioavailability since orally administered drugs could be beneficial [139,140].

Carboxylic/glyoxylic esters and amide-substituted analogs of the **[MnTBAP]$^{3-}$** (Mn(III) 5,10,15,20-tetrakis(4-benzoic acid)-porphyrin) were developed by Gauuan, Day and coworkers [141,142]. While the majority of these complexes showed improved catalase activity, only few analogs of these series showed comparable to improved SOD activity relative to the parent complex. However, it was demonstrated later on how preparations of **[MnTBAP]$^{3-}$** may contain high levels of free manganese impurities (Mn clusters: Mn oxo/hydroxo/acetate) that could be the origin of the SOD activity reported. [93,143] Indeed, this study shows that pure **[MnTBAP]$^{3-}$** is not able to disproportionate superoxide radicals in aqueous media (its SOD activity, if any, is too low to be measured accurately, Table 1) These results underscore again how important is to work with complexes of high purity [86c,93].

Gross and coworkers decided to explore the SOD activity of different metallocorrole complexes based on their previous results that show how the iron and manganese complexes of this type of ligands catalytically decompose peroxynitrite [144,145]. Particularly, they use the 3,17-bis-sulfonated (**MnL15**, Fig. 5) and a series of *ortho*-pyridinium or *para*-pyridinium ring *meso*-substituted corroles (**MnL16–18**, Fig. 5). The electrochemical studies showed how these Mn(III) complexes redox cycle between the Mn(III) and Mn(VI) oxidation states (Table 1), the Mn(II) oxidation state was not observed within the electrochemical window of aqueous solutions. The SOD activity studies, both using the indirect McCord-Fridovich assay and the direct method of pulse radiolysis, showed that all these Mn(III) complexes were active (Table 1). Based on the redox potential values, the authors postulate that the catalytic cycle is initiated by the oxidation of the Mn(III) complex with the subsequent reduction of the superoxide radical (Eq. (3b)) and it is completed by its reduction either by superoxide radical (that oxidizes to oxygen) or hydrogen peroxide (obtaining water and oxygen). The latter was only proven for the corresponding **FeL15** complex. As observed for the porphyrin family, the proximity of positive charge to the metal center enhances SOD activity and the electron-donating/-withdrawing properties of the corrole substituents seem to control the redox potential. Within the series of pyridinium-substituted corroles, a more positive redox potential is observed when more electron-withdrawing ortho-pyridinium rings are present. Contrary to systems that cycle between the Mn(III) and Mn(II) oxidation states, here a negative shift of redox potential will favor SOD activity.

4.4. Acyclic multidentate ligands

Morgenstern-Badarau, Policar and co-workers have been developing manganese complexes of tertiary and secondary amines containing different pendant arms, namely imidazole, pyridine, carboxylate and phenolate (**[MnIPG]$^{+}$**, **[MnBIG]$^{+}$**, **[MnBMPG]$^{+}$**, **[MnL19]$^{+}$**, **[Mn(TMIMA)$_2$]$^{2+}$**, **[Mn(PI)$_2$]$^{2+}$**, Fig. 6) [85,146–148]. These ligands were designed to reproduce the chemical environment found in the active site of the Mn-SOD enzyme, a N_3O_2 set of ligand donors (Fig. 1). In general this family of ligands generated hexacoordinate Mn(II) complexes. Some of these complexes crystallize as helical polymers linked through carboxylato bridges (**[MnIPG]$^{+}$**) or as dimers with either the carboxylate (**[MnBIG]$^{+}$**) or phenolate (**[MnL19]$^{+}$**) ligands acting as bridges [85,148]. However, in aqueous solutions these structures are disrupted leading to monomeric Mn(II) complexes, as shown by EPR and electrochemistry experiments. The complexes **[MnIPG]$^{+}$**, **[MnBIG]$^{+}$**, **[MnBMPG]$^{+}$**, **[Mn(TMIMA)$_2$]$^{2+}$**, and **[Mn(PI)$_2$]$^{2+}$** showed no electrochemical wave in phosphate buffer but irreversible waves were obtained in collidine buffer at pH 7.5, with values ranging from 0.34 to 0.76 V vs. SCE for the anodic potentials and from 0.17 to 0.33 V vs. SCE for the cathodic ones [146]. For **[MnL19]$^{+}$**, the redox process was observed both in PIPES buffer (pH 7.5) with an anodic and cathodic potentials of 0.282 and 0.116 V vs. SCE, respectively, and in phosphate buffer (pH 7.8) with values of 0.334 V and 0.037 vs. SCE, respectively [148]. The reactivity towards the superoxide radical was investigated at pH 7.8 mainly by the McCord-Fridovich indirect method and all the complexes showed SOD activity (Table 1). The reactivity of the complexes **[MnIPG]$^{+}$** and **[MnBIG]$^{+}$** was also studied by pulsed radiolysis and similar values were obtained (Table 1), proving in this way the catalytic nature of the disproportionation of superoxide radicals. A more detailed study of the reactivity of the complex **[MnIPG]$^{+}$** allowed the authors to propose a catalytic mechanism where a transient adduct $\{MnOO\}^6$ ($[Mn(II)OO^{-}]$ or $[Mn(III)OO^{2-}]$) is formed leading subsequently to a Mn(III) complex [147]. Later studies, using low-temperature spectroscopies, support the formation of the $[Mn(III)OO^{2-}]$ [149]. A linear correlation with a negative slope was observed between the anodic potentials and the log $k_{cat(IC50)}$ for these Mn(II) complexes. This indicates that the oxidation of Mn(II) to Mn(III) is the rate-limiting step and thus, the SOD activity would be improved by stabilizing the Mn(III) oxidation state. Indeed, the complex **[Mn(PI)$_2$]$^{2+}$**, that shows one of the highest SOD activity was also isolated in the Mn(III) state [146]. To further lower the redox potential of the Mn(III)/Mn(II) couple, this group designed two new PI-based ligands by introducing an extra carbon in the pedant arm containing the imidazole group, **[Mn(PhIIm)$_2$]$^{+}$** (Fig. 6) and the imine reduced version **[Mn(PhI)$_2$]$^{+}$** [150]. This modification favored a Jahn–Teller tetragonal distortion, as shown by the X-ray crystal structure of **[Mn(PhIIm)$_2$]$^{+}$**, and stabilized the Mn(III) oxidation state. However, these complexes had a lower SOD activity than that observed for the parent complex (Table 1). This could be the result of an excessive stabilization of the Mn(III) state and thus, a harder cycling between the Mn(III) and Mn(II) oxidation sates. The electrochemical experiments did not allow to obtain an estimate of the redox potential associated to the Mn(III)/Mn(II) couple for any of the two complexes.

The group of Guo employed the ligand N,N′-(1,2-phenylene)bis(pyridine-2-carboxaminde) to prepare the complex

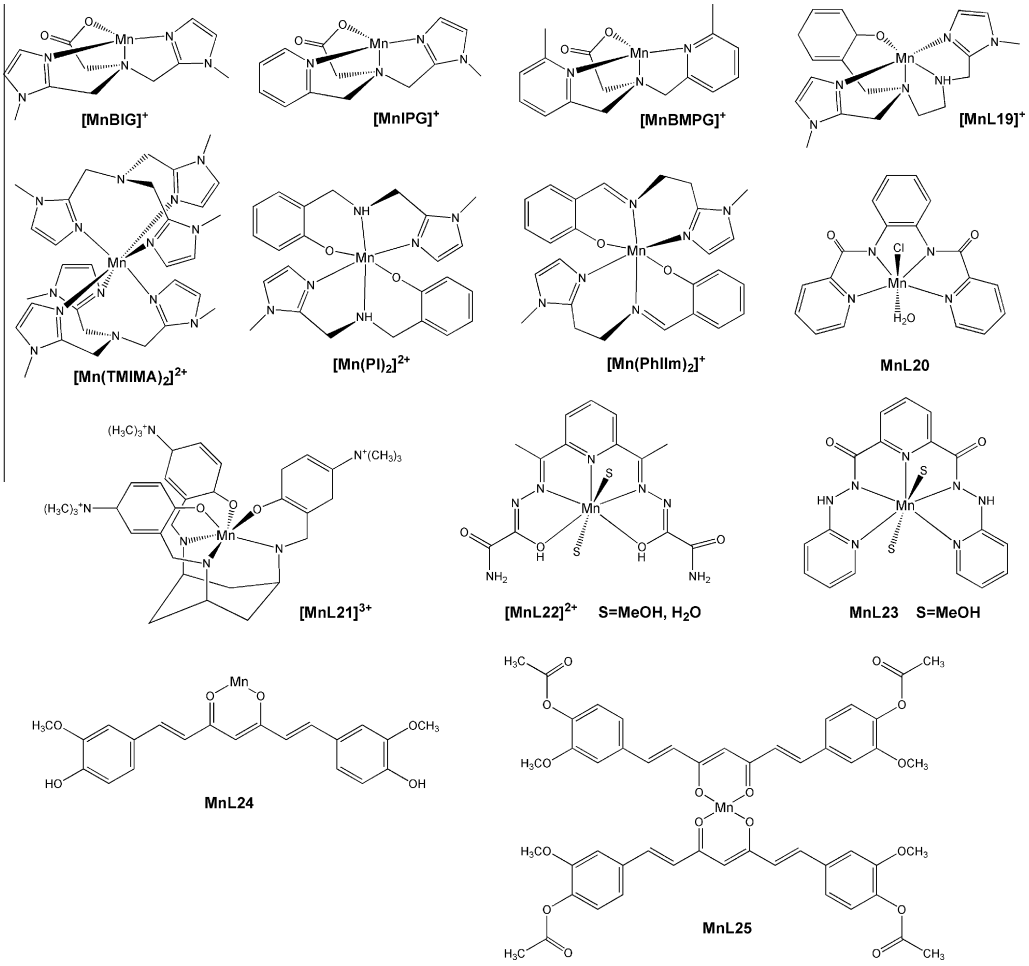

Fig. 6. Schematic of the manganese acyclic multidentate ligand complexes.

MnL20 (Fig. 6) [151]. The X-ray crystal structure showed a Mn(III) with an octahedral geometry coordinated to the four nitrogens of the ligand in the equatorial plane and to one water and chloride ion as axial ligands. Cyclic voltammetry in dimethylformamide showed a reversible Mn(III)/Mn(II) redox process with a half-wave potential value of −0.170 V vs. SCE. Its SOD activity was determined at pH 7.8 by using the riboflavin photoreduction indirect method and an IC_{50} value of 2.93 μM was obtained (Table 1).

Watson and coworkers has used the *cis,cis*-1,3,5,-triaminocylcohexane scaffold to design an aqueous soluble six-coordinate Mn(III) complex, **[MnL21]$^{3+}$** (Fig. 6) [152]. The complex showed SOD activity and the second order rate constant was higher when determined in the absence of catalase (Table 1). This was justified by the presence of hydrogen peroxide in the solution acting as reducing agent and thus facilitating the reduction of Mn(III) to Mn(II). However, the catalase activity of the complex was not explored. A decrease in the rate constant was observed when the ionic strength was increased supporting a rate-determining step which involves species of opposite charges (most likely the superoxide radical and the cationic Mn(III) complex). UV–Vis spectroscopic titrations showed that at pH 8.0 the major species in solution was the monoprotonated **[Mn(L21)H]$^{4+}$**. Authors claim this H^+ could be playing an important role in the mechanism of superoxide radical disproportionation since in the native Mn-SOD both, electron and proton transfer, are involved in the reaction. Electrochemical studies in dimethylformamide revealed two quasi-reversible metal-center redox processes, Mn(IV)/Mn(III) and Mn(III)/Mn(II) with $E_{1/2}$ values of 0.51 V and −0.07 V vs. NHE, respectively (Table 1). Although both redox couples could be participating in the reaction, Mn(III)/Mn(II) is supported as the actual active one based on the effect that hydrogen peroxide has in the SOD activity.

Ivanovic-Burmazovic group has shown how seven-coordinate Mn(II) complexes of the acyclic and rigid H_2dapsox (2,6-diacetylpyridine(semioxamazide)) (**[MnL22]$^{2+}$**) and H_2Dcphp (N'^2, N'^6-di(pyridin-2-yl)pyridine-2,6-dicarbohydrazide) (**MnL23**) ligands are very efficient in catalyzing the disproportionation of superoxide radicals, with catalytic rate constants of 1.2×10^7 M^{-1} s^{-1} and 6.1×10^6 M^{-1} s^{-1}, respectively (Table 1) [102,153]. These values were determined by using direct stopped-flow measurements in dimethyl sulfoxide (0.06% water). The reactivity of the complex **[MnL22]$^{2+}$** was also studied in aqueous media at pH 7.8 (phosphate buffer) using the indirect McCord-Fridovich assay and a rate constant one order of magnitude higher was obtained (1.9×10^8 M^{-1} s^{-1}, IC_{50} of 0.013 μM Table 1). This higher value was the result of a direct reaction between **[MnL22]$^{2+}$** and the indicator cyt *c* (the oxidized form of the complex reoxidized the reduced cyt *c*) [102]. When NBT was used as indicator, no SOD activity was detected due to the formation of a complex between NBT and **[MnL22]$^{2+}$** that precipitated from solution. These results highlight how indirect methods could not always be reliable and can only be applied upon considering possible cross-reactions that can occur at the same time in solution. Both Mn(II) complexes, **[MnL22]$^{2+}$** and **MnL23**, show a distorted pentagonal-bipyramidal geometry with the pentadentate ligand coordinated in the equatorial plane and two solvent molecules (water or methanol) in the axial positions

[102,153]. Interestingly, the H_2Daphp (2,6-bis((2-(pyridin-2-yl)hydrazono)ethyl)pyridine) ligand binds Mn(II) with the same overall geometry but shows no SOD activity [153]. While the two complexes **[MnL22]$^{2+}$** and **MnL23** have redox potentials values of 0.37 V and 0.66 V vs. Ag/AgCl, respectively, the Mn(II) complex of H_2Daphp showed no signal in the scan range from −1 to 1.2 V, which is indicative of a high redox potential (>1.2 V). Despite the similarity of the ligands H_2Daphp and H_2Dcphp, their redox properties are very different. Authors claimed that the simple modification, hydrazone (imino nitrogen) vs. hydrazide (amido nitrogen), led in the latter case to negatively charge amido nitrogens upon Mn(II) coordination (**MnL23**, Fig. 6), a key factor since their strong sigma-donor ability can stabilize the Mn(III) oxidation state decreasing the Mn(III)/Mn(II) redox potential by at least 0.8 V. These results show how the redox activity of manganese complexes can be modulated without changing the donor set and coordination geometry, as demonstrated previously for other manganese systems [125,126,129,154–156]. In addition, they suggest that solvent dissociation and formation of a six-coordinate intermediate are not crucial for SOD activity (see Section 4.1).

Vajragupta and coworkers have explored how Mn(II) coordination can enhance the antioxidant properties of curcumin and its diacetyl derivative [83]. Both Mn(II) complexes (**MnL24** and **MnL25**, Fig. 6) showed higher SOD activity than the precursors as determined by the McCord-Fridovich indirect method using NBT (IC_{50} values of 29.9 and 24.7 μM for **MnL24** and **MnL25**, respectively, Table 1). Curcumin inhibited only 18.6% of NBT at 270 μM whereas the diacetyl derivative showed no inhibition at this concentration. A lower SOD activity was determined by using the spin trap DMPO as indicator (**MnL24**: $IC_{50,DMPO} = 1.09 \times 10^{-3}$ μM ($k_{cat} = 6.9 \times 10^3$ $M^{-1}\,s^{-1}$) and **MnL25**: 2.40×10^{-3} μM ($k_{cat} = 3.1 \times 10^3$ $M^{-1}\,s^{-1}$). Stability studies in water at different pH values revealed that these complexes release around 40% Mn(II) at pH 7.4. Thus, although the authors added EDTA (up to 5%) or albumin (up to 1.6%) in the solution when determining the SOD activity and the results were not considerably different, the amount of remaining free Mn(II) could be the source of the SOD activity. Thus, it is not completely clear whether these complexes have SOD activity by themselves or whether the released Mn(II) is acting as the active species. Release of Mn(II) was also detected in human blood/serum. No redox properties were reported.

4.5. Peptide based-ligands

Using the *de novo* peptide/protein design approach, the group of Singh and coworkers has prepared an helix-loop-helix polypeptide containing the four amino acids that define the active center of the native Mn-SOD (three His and one Asp, Fig. 1) [157]. EPR experiments at pH 8.0 indicated that the peptide bound one Mn(II) with a K_d of 36 μM. Authors propose that Mn(II) is bound to the designed site, i.e. non-specific binding observed, since for the corresponding peptide missing one His and the Asp no binding was observed. The SOD activity was evaluated at pH 7.4 (50 mM potassium phosphate) and an IC_{50} value of 8.08 μM was obtained (**MnL26**, Table 1). Based on the fact that neither the apo-peptide nor the pure Mn(II) showed any activity, the authors suggest that the observed SOD activity is due to the Mn(II)-peptide complex. Interesting, Mn(II) ions have been reported to have SOD activity under the experimental conditions used here [79,88].

5. Conclusions

Different manganese complexes, containing either Mn(II) or Mn(III), have been designed and reported to show SOD activity *in vitro* (Table 1), with some complexes displaying also activity *in vivo*. Interestingly, the majority of them do not present neither the donor set of ligands or atoms (three histidines and one aspartic acid = three nitrogens and one oxygen) neither the coordination geometry (distorted trigonal bipyramidal, Fig. 1) found in the active center of the native Mn-SOD enzyme. However, all of them have a redox potential ($E_{1/2}$, Table 1) in between the redox potentials corresponding to the reduction (0.89 V vs. NHE, 0.65 V vs. SCE) and oxidation (−0.16 V vs. NHE, −0.40 V vs. SCE) of the superoxide radical [45]. Complexes with $E_{1/2}$ close to 0.36 V vs. NHE (0.12 vs. SCE), the intermediate value between the above potentials, display higher SOD activity independently if the redox cycle occurs between the oxidation states Mn(III)/Mn(II) or Mn(IV)/Mn(III). This is indicative of how crucial is to fine-tune the redox activity of the manganese ion for the function as SOD catalytic center. Although the redox potential values are not available for all the manganese complexes reported here and the SOD activity was determined under different conditions, a general trend is observed where for complexes with low $E_{1/2}$ the SOD activity increases as the $E_{1/2}$ values raise (indicating that the reduction of the Mn(III) or Mn(IV) is the rate-determining step) reaching a certain value where the reduced state of the metal is stabilized and then a decrease in rate is observed as the $E_{1/2}$ increases (the oxidation of the Mn(II) or Mn(III) has become the rate-determining step) [93,120,132,146,153]. The higher SOD activity is observed when the reduction and oxidation of the metal center by the superoxide radical proceed at similar rates. Exceptions are observed that call for different mechanisms where the redox control, even being an important factor, is not defining the rate-determining step of the catalytic process, and other elements, such as the coordination geometry preferences for different oxidation sates and/or intermediates, and level of flexibility of the ligand, could govern the SOD reactivity [106]. A common theme of the most effective SOD mimics is the presence of positive charges that guide the superoxide radical to the reactive metal center. This electrostatic guidance is a known key factor in the native enzymes [10,42].

With the exception of a few families of complexes [89–93], *in vivo* studies are still very limited. The results obtained so far highlight the fact that there is not always a direct correlation between *in vitro* and *in vivo* studies. The parameters governing the SOD activity in both situations could be completely different. Factors such a lipophilicity and right biodistribution (cellular location) can compensate for lower SOD activities. Thus, depending on the electrostatic, steric, solvation, lipophilicity and stability properties of these complexes, different potency can be expected between the *in vitro* and *in vivo* results. More studies to understand the pharmacokinetics of these complexes are definitely needed. Stability under physiological conditions is another key factor because the release of Mn(II) would give false positive results since Mn(II) itself shows SOD activity. Indeed, this has already been proposed to be the case for several Mn(II) complexes reported to be active [79,87,88]. Control experiments where the activity of the ligands themselves and Mn(II) are studied are fundamental. More importantly, the purity of the complexes employed is critical to avoid artifacts and misleading results [86,93]. Finally, considering that due to their intrinsic nature these complexes react or have the potential to react with other ROS (i.e. hydrogen peroxide and hydroxyl radicals) and RNS (i.e. peroxynitrite) species, specially when tested *in vivo*, further work is required to gain insight into their reactivity and mode of action. If specificity for superoxide radicals may be desirable for mechanistic studies, the ability to eliminate different ROS or RNS can be beneficial for therapeutic uses. The understanding of the reactions of superoxide radical with metal centers will help in conceiving whether and how metal complexes can be used as pharmaceuticals for treatment of disease states caused by this radical overproduction. Moreover, this knowledge can guide the

design of ligands with a wide range of possibilities for fine-tuning the metal redox potential and the overall charge and lipophilicity.

Acknowledgments

O.I. thanks the Fundação para a Ciência e a Tecnologia (FCT) for a Ciência 2007 Grant and the European Commission for a Marie Curie IRG fellowship (FP7-IRG).

References

[1] M.J. Green, H.A.O. Hill, Methods Enzymol. 105 (1984) 93–104.
[2] A.-F. Miller, D.L. Sorkin, Comments Mol. Cell. Biophys. 9 (1997) 1–48.
[3] A.-F. Miller, in: L.J. Que, W. Tolman (Eds.), Comprehensive Coordination Chemistry II, Coordination Chemistry in the Biosphere and Geosphere, vol. 8, Elsevier Ltd., 2003, pp. 479–506.
[4] C. Szabo, Toxicol. Lett. 140–141 (2003) 105–112.
[5] C. Szabo, H. Ischiropoulos, R. Radi, Nat. Rev. Drug. Discov. 6 (2007) 662–680.
[6] H.M. Hassan, I. Fridovich, Eur. J. Rheumatol. Inflamm. 4 (1981) 160–172.
[7] I. Fridovich, Annu. Rev. Biochem. 64 (1995) 97–112.
[8] J.M. McCord, I. Fridovich, J. Biol. Chem. 244 (1969) 6049–6055.
[9] I.A. Abreu, D.E. Cabelli, Biochim. Biophys. Acta (BBA) – Proteins Proteomics 1804 (2010) 263–274.
[10] J.J.P. Perry, D.S.Shin, E.D. Getzoff, J.A. Tainer, Biochim. Biophys. Acta (BBA) – Proteins Proteomics 1804 (2010) 245–262.
[11] G.A. Keller, T.G. Warner, K.S. Steimer, R.A. Hallewell, Proc. Natl. Acad. Sci. USA 88 (1991) 7381–7385.
[12] J.D. Crapo, T. Oury, C. Rabouille, J.W. Slot, L.Y. Chang, Proc. Natl. Acad. Sci. USA 89 (1992) 10405–10409.
[13] S.L. Marklund, Biochem. J. 222 (1984) 649–655.
[14] R.A. Weisiger, I. Fridovich, J. Biol. Chem. 248 (1973) 4793–4796.
[15] J.S. Valentine, D.L. Wertz, T.J. Lyons, L.-L. Liou, J.J. Goto, E.B. Gralla, Curr. Opin. Chem. Biol. 2 (1998) 253–262.
[16] C.M. Maier, P.H. Chan, The Neuroscientist 8 (2002) 323–334.
[17] D. Kumar, B.I. Jugdutt, J. Lab. Clin. Med. 142 (2003) 288–297.
[18] H.K. Saini, J. Machackova, N.S. Dhalla, Antioxid. Redox Signal. 6 (2004) 393–404.
[19] S.C. Fagan, D.C. Hess, E.J. Hohnadel, D.M. Pollock, A. Ergul, Stroke 35 (2004) 2220–2225.
[20] J.M. McCord, J. Free Radical Biol. Med. 2 (1986) 307–310.
[21] S.W. Werns, P.J. Simpson, J.K. Mickelson, M.J. Shea, B. Pitt, B. Lucchesi, J. Cardiovasc. Pharmacol. 11 (1988) 36–44.
[22] B.A. Omar, J.M. McCord, J. Mol. Cell Cardiol. 23 (1991) 149–159.
[23] Y. Ando, M. Inoue, M. Hirota, Y. Morino, S. Araki, Brain Res. 477 (1989) 286–291.
[24] P.H. Chan, G.Y. Yang, S.F. Chen, E. Carlson, C.J. Epstein, Ann. Neurol. 29 (1991) 482–486.
[25] G.Y. Yang, P.H. Chan, J. Chen, E. Carlson, S.F. Chen, P. Weinstein, C.J. Epstein, H. Kamii, Stroke 25 (1994) 165–170.
[26] J.W. Francis, J. Ren, L. Warren, R.H. Brown, S.P. Finklestein, Exp. Neurol. 146 (1997) 435–443.
[27] K. Pong, Expert Opin. Biol. Ther. 3 (2003) 127–139.
[28] M. Shingu, S. Takahashi, M. Ito, N. Hamamatu, Y. Suenaga, Y. Ichibangase, Rheumatol. Int. 14 (1994) 77–81.
[29] S. Church, J.W. Grant, L.A. Ridnour, L.W. Oberley, P.E. Swanson, P.S. Meltzer, J.M. Trent, Proc. Natl. Acad. Sci. USA 90 (1993) 3113–3117.
[30] N. Yoshizaki, Y. Mogi, H. Muramatsu, K. Koike, K. Kogawa, Y. Niitsu, Int. J. Cancer 57 (1994) 287–292.
[31] P. Wardman, L.P. Candeias, Radiat. Res. 145 (1996) 523–531.
[32] C. Walling, Acc. Chem. Res. 8 (1975) 125–131.
[33] J. Prousek, Pure Appl. Chem. 79 (2007) 2325–2338.
[34] F.S. Archibald, I. Fridovich, J. Bacteriol. 145 (1981) 442–451.
[35] E.C. Chang, D.J. Kosman, J. Biol. Chem. 264 (1989) 12172–12178.
[36] M. Al-Maghrebi, I. Fridovich, L. Benov, Arch. Biochem. Biophys. 402 (2002) 104–109.
[37] M.J. Daly, E.K. Gaidamakova, V.Y. Matrosova, A. Vasilenko, M. Zhai, A. Venkateswaran, M. Hess, M.V. Omelchenko, H.M. Kostandarithes, K.S. Makarova, L.P. Wackett, J.K. Fredrickson, D. Ghosal, Science 306 (2004) 1025–1028.
[38] A.R. Reddi, L.T. Jensen, A. Naranuntarat, E. Rosenfeld, E. Leung, R. Shah, V.C. Culotta, Free Radical Biol. Med. 46 (2009) 154–162.
[39] B.B. Keele, J.M. McCord, I. Fridovich, J. Biol. Chem. 245 (1970) 6176–6181.
[40] A.-F. Miller, in: A. Messerschmidt, R. Huber, K. Wieghardt, T. Poulos, M. Cygler, W. Bode (Eds.), Handbook of Metalloproteins, John Wiley & Sons, Chichester, 2001, pp. 668–682.
[41] E.M. Stroupe, M. DiDonato, J.A. Tainer, in: A. Messerschmidt, R. Huber, K. Wieghardt, T. Poulos, M. Cygler, W. Bode (Eds.), Handbook of Metalloproteins, John Wiley & Sons, Chichester, 2003, pp. 941–951.
[42] J. Sines, S. Allison, A. Wierzbicki, J.A. McCammon, J. Phys. Chem. 94 (1990) 959–961.
[43] C. Bull, J.A. Fee, J. Am. Chem. Soc. 107 (1985) 3295–3304.
[44] A.-F. Miller, K. Padmakumar, D.L. Sorkin, A. Karapetian, C.K. Vance, J. Inorg. Biochem. 93 (2003) 71–83.
[45] D.T. Sawyer, J.S. Valentine, Acc. Chem. Res. 14 (1981) 393–400.
[46] W.C.J. Barrette, D.T. Sawyer, J.A. Fee, K. Asada, Biochemistry 22 (1983) 624–627.
[47] L.M. Ellerby, D.E. Cabelli, J.A. Graden, J.S. Valentine, J. Am. Chem. Soc. 118 (1996) 6556–6561.
[48] G.D. Lawrence, D.T. Sawyer, Biochemistry 18 (1979) 3045–3050.
[49] V.J.-P. Leveque, C.K. Vance, H.S. Nick, D.N. Silverman, Biochemistry 40 (2001) 10586–10591.
[50] C.K. Vance, A.-F. Miller, J. Am. Chem. Soc. 120 (1998) 461–467.
[51] A.-F. Miller, Acc. Chem. Res. 41 (2008) 501–510.
[52] B. Meier, D. Barra, F. Bossa, L. Calabrese, G. Rotilio, J. Biol. Chem. 257 (1982) 13977–13980.
[53] M.E. Martin, B.R. Byers, M.O. Olson, M.L. Salin, J.E. Arceneaux, C. Tolbert, J. Biol. Chem. 261 (1986) 9361–9367.
[54] C.D. Pennington, E.M. Gregory, J. Bacteriol. 166 (1986) 528–532.
[55] A. Amano, S. Shizukuishi, H. Tamagawa, K. Iwakura, S. Tsunasawa, A. Tsunemitsu, J. Bacteriol. 172 (1990) 1457–1463.
[56] L.C. Tabares, C. Bittel, N. Carrillo, A. Bortolotti, N. Cortez, J. Bacteriol. 185 (2003) 3223–3227.
[57] D.E. Ose, I. Fridovich, J. Biol. Chem. 251 (1976) 1217–1218.
[58] F. Yamakura, J. Biochem. 83 (1978) 849–857.
[59] F. Yamakura, K. Suzuki, J. Biochem. 88 (1980) 191–196.
[60] T.A. Jackson, T.C. Brunold, Acc. Chem. Res. 37 (2004) 461–470.
[61] L.E. Grove, T.C. Brunold, Comments Inorg. Chem. 29 (2008) 134–168.
[62] L.C. Tabares, J. Gätjens, S. Un, Biochim. Biophys. Acta (BBA) – Proteins Proteomics 1804 (2010) 308–317.
[63] H.A. Schwarz, J. Chem. Educ. 58 (1981) 101–105.
[64] S. Goldstein, C. Michel, W. Bors, M. Saran, G. Czapski, Free Radical Biol. Med. 4 (1988) 295–303.
[65] D. Klug-Roth, I. Fridovich, J. Rabani, J. Am. Chem. Soc. 95 (1973) 2786–2790.
[66] J.S. Valentine, A.R. Miksztal, D.T. Sawyer, Methods Enzymol. 105 (1984) 71–81.
[67] D.P. Riley, W.J. Rivers, R.H. Weiss, Anal. Biochem. 196 (1991) 344–349.
[68] R.H. Weiss, A.G. Flickinger, W.J. Rivers, M.M. Hardy, K.W. Aston, U.S. Ryan, D.P. Riley, J. Biol. Chem. 268 (1993) 23049–23054.
[69] D.-H. Chin, G.J. Chiericato, D.T. Sawyer, J. Am. Chem. Soc. 104 (1982) 1296–1299.
[70] (a) L. Flohe, F. Otting, Methods Enzymol. 105 (1984) 93–104;
(b) S.I. Liochev, I. Fridovich, Arch. Biochem. Biophys. 318 (1995) 408–410;
(c) B. Halliwell, J.M.C. Gutteridge, Free Radicals in Biology and Medicine, fourth ed., Oxford University Press, New York, 2007.
[71] H. Ukeda, S. Maeda, T. Ishii, M. Sawamura, Anal. Biochem. 251 (1997) 206–209.
[72] M.W. Sutherland, B.A. Learmonth, Free Radical Res. 27 (1997) 283–289.
[73] H. Ukeda, D. Kawana, S. Maeda, M. Sawamura, Biosci. Biotechnol. Biochem. 63 (1999) 485–488.
[74] B. Gray, A.J. Carmichael, Biochem. J. 281 (1992) 795–802.
[75] S. Marklund, G. Marklund, Eur. J. Biochem. 47 (1974) 469–474.
[76] G. Cohen, R.E. Heikkila, J. Biol. Chem. 249 (1974) 2447–2452.
[77] H.P. Misra, I. Fridovich, J. Biol. Chem. 247 (1972) 3170–3175.
[78] C. Beauchamp, I. Fridovich, Anal. Biochem. 44 (1971) 276–287.
[79] K. Barnese, E.B. Gralla, D.E. Cabelli, J.S. Valentine, J. Am. Chem. Soc. 130 (2008) 4604–4606.
[80] Y. Sawada, I. Yamazaki, Biochim. Biophys. Acta 327 (1973) 257–265.
[81] B.H.J. Bielski, H.W. Richter, J. Am. Chem. Soc. 99 (1977) 3019–3023.
[82] J. Butler, W.H. Koppenol, E. Margoliash, J. Biol. Chem. 257 (1982) 10747–10750.
[83] O. Vajragupta, P. Boonchoong, L.J. Berliner, Free Radical Res. 38 (2004) 303–314.
[84] J.-L. Pierre, P. Chautemps, R. Sidi, C. Beguin, A. El Marzouki, G. Serratrice, E. Saint-Aman, P. Rey, J. Am. Chem. Soc. 117 (1995) 1965–1973.
[85] C. Policar, S. Durot, F. Lambert, M. Cesario, F. Ramiandrasoa, I. Morgenstern-Badarau, Eur. J. Inorg. Chem. (2001) 1807–1818.
[86] (a) W. Munroe, C. Kingsley, A. Durazo, E. Butler Gralla, J.A. Imlay, C. Srinivasan, J.S. Valentine, J. Inorg. Biochem. 101 (2007) 1875–1882;
(b) J.M. Pollard, J.S. Rebouças, A. Durazo, I. Kos, F. Fike, M. Panni, E.B. Gralla, J.S. Valentine, I. Batinić-Haberle, R.A. Gatti, Free Radical Biol. Med. 47 (2009) 250–260;
(c) J.S. Rebouças, I. Spasojević, I. Batinić-Haberle, J. Pharm. Biomed. Anal. 48 (2008) 1046–1049.
[87] J.S. Rebouças, G. DeFreitas-Silva, I. Spasojević, Y.M. Idemori, L. Benov, I. Batinić-Haberle, Free Radical Biol. Med. 45 (2008) 201–210.
[88] I. Spasojević, I. Batinić-Haberle, R.D. Stevens, P. Hambright, A.N. Thorpe, J. Grodkowski, P. Neta, I. Fridovich, Inorg. Chem. 40 (2001) 726–739.
[89] S.R. Doctrow, K. Huffman, C.B. Marcus, W. Musleh, A. Bruce, M. Baudry, B. Malfroy, in: H. Sies (Ed.), Antioxidants in Disease Mechanisms and Therapeutic Strategies, Academic Press, 1997, pp. 247–269.
[90] D.P. Riley, Chem. Rev. 99 (1999) 2573–2587.
[91] S.L. Henke, Exp. Opin. Ther. Patents 9 (1999) 169–180.
[92] C. Muscoli, S. Cuzzocrea, D.P. Riley, J.L. Zweier, C. Thiemermann, Z.-Q. Wang, D. Salvemini, Brit. J. Pharmacol. 140 (2003) 445–460.
[93] (a) I. Batinić-Haberle, J.S. Rebouças, I. Spasojević, Antioxid. Redox Signal. 13 (2010) 877–918;
(b) I. Batinić-Haberle, I. Spasojević, H.M. Tse, A. Tovmasyan, Z. Rajic, D.K. St. Clair, Z. Vujasković, M.W. Dewhirst, J.D. Piganelli, Amino Acids (2010) 1–19. doi:10.1007/s00726-010-0603-6.

[94] D.P. Riley, Adv. Supramol. Chem. 6 (2000) 217–244.
[95] D.P. Riley, O.F. Schall, Adv. Inorg. Chem. 59 (2007) 233–263.
[96] D. Salvemini, Z.-Q. Wang, J.L. Zweier, A. Samouilov, H. Macarthur, T.P. Misko, M.G. Currie, S. Cuzzocrea, J.A. Sikorski, D.P. Riley, Science 286 (1999) 304–306.
[97] K. Aston, N. Rath, A. Naik, U. Slomczynska, O.F. Schall, D.P. Riley, Inorg. Chem. 40 (2001) 1779–1789.
[98] M. Di Napoli, F. Papa, IDrugs 8 (2005) 67–76.
[99] D.P. Riley, R.H. Weiss, J. Am. Chem. Soc. 116 (1994) 387–388.
[100] D.P. Riley, P.J. Lennon, W.L. Neumann, R.H. Weiss, J. Am. Chem. Soc. 119 (1997) 6522–6528.
[101] A. Dees, A. Zahl, R. Puchta, N.J.R. van Eikema Hommes, F.W. Heinemann, I. Ivanović-Burmazović, Inorg. Chem. 46 (2007) 2459–2470.
[102] G.-F. Liu, M. Filipovic, F.W. Heinemann, I. Ivanović-Burmazović, Inorg. Chem. 46 (2007) 8825–8835.
[103] I. Ivanović-Burmazović, R. van Eldik, Dalton Trans. 39 (2008) 5259–5275.
[104] M.R. Filipovic, K. Duerr, M. Mojovic, V. Simeunovic, R. Zimmermann, V. Niketic, I. Ivanović-Burmazović, Angew. Chem. Int. Ed. 47 (2008) 8735–8739.
[105] M.R. Filipovic, A.C.W. Koh, S. Arbault, V. Niketic, A. Debus, U. Schleicher, C. Bogdan, M. Guille, F. Lemaitre, C. Amatore, I. Ivanović-Burmazović, Angew. Chem. Int. Ed. 49 (2010) 4228–4232.
[106] A. Maroz, G.F. Kelso, R.A. Smith, D.C. Ware, R.F. Anderson, J. Phys. Chem. A 112 (2008) 4929–4935.
[107] Q.-X. Li, Q.-H. Luo, Y.-Z. Li, Z.-Q. Pan, M.-C. Shen, Eur. J. Inorg. Chem. (2004) 4447–4456.
[108] P. Failli, D. Bani, A. Bencini, M. Cantore, L. Di Cesare Mannelli, C. Ghelardini, C. Giorgi, M. Innocenti, F. Rugi, A. Spepi, R. Udisti, B. Valtancoli, J. Med. Chem. 52 (2009) 7273–7283.
[109] J.O. Bockris, A.K.N. Reddy, M.G. Aldeco, Modern Electrochemistry, Kluwer Academic Plenum Publishers, New York, 2000.
[110] M. Baudry, S. Etienne, A. Bruce, M. Palucki, E. Jacobsen, B. Malfroy, Biochem. Biophys. Res. Commun. 192 (1993) 964–968.
[111] S. Melov, J. Ravenscroft, S. Malik, M.S. Gill, D.W. Walker, P.E. Clayton, D.C. Wallace, B. Malfroy, S.R. Doctrow, G.J. Lithgow, Science 289 (2000) 1567–1569.
[112] S. Melov, S.R. Doctrow, J.A. Schneider, J. Haberson, M. Patel, P.E. Coskun, K. Huffman, D.C. Wallace, B. Malfroy, J. Neurosci. 21 (2001) 8348–8353.
[113] F. Fucassi, J.E. Lowe, K.D. Pavey, S. Shah, R.G.A. Faragher, M.H.L. Green, F. Paul, D. O'Hare, P.J. Cragg, J. Inorg. Biochem. 101 (2007) 225–232.
[114] G.M.P. Giblin, P.C. Box, I.B. Campbell, A.P. Hancock, S. Roomans, G.I. Mills, C. Molloy, G.E. Tranter, A.L. Walker, S.R. Doctrow, K. Huffman, B. Malfroy, Bioorg. Med. Chem. Lett. 11 (2001) 1367–1370.
[115] S.R. Doctrow, K. Huffman, C.B. Marcus, G. Tocco, E. Malfroy, C.A. Adinolfi, H. Kruk, K. Baker, N. Lazarowych, J. Mascarenhas, B. Malfroy, J. Med. Chem. 45 (2002) 4549–4558.
[116] R. Liu, Y. Ingrid, X. Bi, R.F. Thompson, S.R. Doctrow, B. Malfroy, M. Baudry, Proc. Natl. Acad. Sci. USA 100 (2003) 8526–8531.
[117] S.R. Doctrow, M. Baudry, K. Huffman, B. Malfroy, S. Melov, in: Medicinal Inorganic Chemistry, American Chemical Society Series: Models for Neurodegenerative Diseases of Aging, 2005, pp. 319–347.
[118] W. Park, D. Lim, Bioorg. Med. Chem. Lett. 19 (2009) 614–617.
[119] A. Puglisi, G. Tabbì, G. Vecchio, J. Inorg. Biochem. 98 (2004) 969–976.
[120] D. Moreno, V. Daier, C. Palopoli, J.-P. Tuchagues, S. Signorella, J. Inorg. Biochem. 104 (2010) 496–502.
[121] V. Daier, D. Moreno, C. Duhayon, J.-P. Tuchagues, S. Signorella, Eur. J. Inorg. Chem. (2010) 965–974.
[122] K. Ghosh, N. Tyagi, P. Kumar, U.P. Singh, N. Goel, J. Inorg. Biochem. 104 (2010) 9–18.
[123] R.F. Pasternack, A. Banth, J.M. Pasternack, C.S. Johnson, J. Inorg. Biochem. 15 (1981) 261–267.
[124] R. Kachadourian, I. Batinić-Haberle, I. Fridovich, Inorg. Chem. 38 (1999) 391–396.
[125] I. Batinić-Haberle, I. Spasojević, P. Hambright, L. Benov, A.L. Crumbliss, I. Fridovich, Inorg. Chem. 38 (1999) 4011–4022.
[126] I. Spasojević, I. Batinić-Haberle, Inorg. Chim. Acta 317 (2001) 230–242.
[127] I. Batinić-Haberle, L. Benov, I. Spasojević, I. Fridovich, J. Biol. Chem. 273 (1998) 24521–24528.
[128] I. Spasojević, I. Batinić-Haberle, J.S. Rebouças, Y.M. Idemori, I. Fridovich, J. Biol. Chem. 278 (2003) 6831–6837.
[129] J.S. Rebouças, I. Spasojević, D.H. Tjahjono, A. Richaud, F. Mendez, L. Benov, I. Batinić-Haberle, Dalton Trans. (2008) 1233–1242.
[130] I. Batinić-Haberle, I. Spasojević, R.D. Stevens, P. Hambright, I. Fridovich, J. Chem. Soc., Dalton Trans. (2002) 2689–2696.
[131] R. Kachadourian, I. Batinić-Haberle, I. Fridovich, Free Radical Biol. Med. 25 (Supplement 1) (1998) S17.
[132] I. Batinić-Haberle, I. Spasojević, R.D. Stevens, P. Hambright, P. Neta, A. Okado-Matsumoto, I. Fridovich, Dalton Trans. (2004) 1696–1702.
[133] A. Okado-Matsumoto, I. Batinić-Haberle, I. Fridovich, Free Radical Biol. Med. 37 (2004) 401–410.
[134] I. Batinić-Haberle, I. Spasojević, R.D. Stevens, B. Bondurant, A. Okado-Matsumoto, I. Fridovich, Z. Vujasković, M.W. Dewhirst, Dalton Trans. (2006) 617–624.
[135] I. Spasojević, Y. Chen, T.J. Noel, Y. Yu, M.P. Cole, L. Zhang, Y. Zhao, D.K. St. Clair, I. Batinić-Haberle, Free Radical Biol. Med. 42 (2007) 1193–1200.
[136] H. Sheng, W. Yang, S. Fukuda, H.M. Tse, W. Paschen, K. Johnson, I. Batinić-Haberle, J.D. Crapo, R.D. Pearlstein, J. Piganelli, D.S. Warner, Free Radical Biol. Med. 47 (2009) 917–923.
[137] D. Lahaye, K. Muthukumaran, C.-H. Hung, D. Gryko, J.S. Rebouças, I. Spasojević, I. Batinić-Haberle, J.S. Lindsey, Bioorg. Med. Chem. 15 (2007) 7066–7086.
[138] I. Kos, L. Benov, I. Spasojević, J.S. Rebouças, I. Batinić-Haberle, J. Med. Chem. 52 (2009) 7868–7872.
[139] L.-P. Liang, J. Huang, R. Fulton, B.J. Day, M. Patel, J. Neurosci. 27 (2007) 4326–4333.
[140] R. Rosenthal, R. Rosenthal, K. Huffman, L. Fisette, C. Damphousse, W. Callaway, B. Malfroy, S.R. Doctrow, J. Biol. Inorg. Chem. 14 (2009) 979–991.
[141] P.J.F. Gauuan, M.P. Trova, L. Gregor-Boros, S.B. Bocckino, J.D. Crapo, B.J. Day, Bioorg. Med. Chem. 10 (2002) 3013–3021.
[142] M.P. Trova, P.J.F. Gauuan, A.D. Pechulis, S.M. Bubb, S.B. Bocckino, J.D. Crapo, B.J. Day, Bioorg. Med. Chem. 11 (2003) 2695–2707.
[143] J.S. Rebouças, I. Spasojević, I. Batinić-Haberle, J. Biol. Inorg. Chem. 13 (2008) 289–302.
[144] A. Mahammed, Z. Gross, Angew. Chem. Int. Ed. 45 (2006) 6544–6547.
[145] M. Eckshtain, I. Zilbermann, A. Mahammed, I. Saltsman, Z. Okun, E. Maimon, H. Cohen, D. Meyerstein, Z. Gross, Dalton Trans. (2009) 7879–7882.
[146] S. Durot, C. Policar, F. Cisnetti, F. Lambert, J.-P. Renault, G. Pelosi, G. Blain, H. Korri-Youssoufi, J.-P. Mahy, Eur. J. Inorg. Chem. (2005) 3513–3523.
[147] S. Durot, F. Lambert, J.-P. Renault, C. Policar, Eur. J. Inorg. Chem. (2005) 2789–2793.
[148] F. Cisnetti, A.-S. Lefèvre, R. Guillot, F. Lambert, G. Blain, E. Anxolabéhère-Mallart, C. Policar, Eur. J. Inorg. Chem. (2007) 4472–4480.
[149] S. Groni, G. Blain, R. Guillot, C. Policar, E. Anxolabéhère-Mallart, Inorg. Chem. 46 (2007) 1951–1953.
[150] F. Cisnetti, G. Pelosi, C. Policar, Inorg. Chim. Acta 360 (2007) 557–562.
[151] J. Lin, C. Tu, H. Lin, P. Jiang, J. Ding, Z. Guo, Inorg. Chem. Commun. 6 (2003) 262–265.
[152] E.A. Lewis, H.H. Khodr, R.C. Hider, J.R. Lindsay Smith, P.H. Walton, Dalton Trans. (2004) 187–188.
[153] G.-F. Liu, K. Durr, R. Puchta, F.W. Heinemann, R. van Eldik, I. Ivanović-Burmazović, Dalton Trans. (2009) 6292–6295.
[154] E.A. Lewis, J.R. Lindsay Smith, P.H. Walton, S.J. Archibald, S.P. Foxon, G.M.P. Giblin, J. Chem. Soc. Dalton Trans. (2001) 1159–1161.
[155] J. Gätjens, M. Sjodin, V.L. Pecoraro, S. Un, J. Am. Chem. Soc. 129 (2007) 13825–13827.
[156] M. Sjodin, J. Gätjens, L.C. Tabares, P. Thuery, V.L. Pecoraro, S. Un, Inorg. Chem. 47 (2008) 2897–2908.
[157] U. Singh, R. Singh, Y. Isogai, Y. Shiro, Int. J. Pept. Res. Ther. 12 (2006) 379–385.
[158] J.A. Fee, P.E. DiCorleto, Biochemistry 12 (1973) 4893–4899.